ADSORPTION OF LEAD (Pb) IN WATER USING BIOCHAR AND BIOCHAR-ALGINATE COMPOSITE BEADS

by

Charlie Parent

Submitted in partial fulfilment of the requirements
for the degree of Master of Science

at

Dalhousie University
Halifax, Nova Scotia
June, 2023

Dalhousie University is located in Mi'kma'ki, the
ancestral and unceded territory of the Mi'kmaq.
We are all Treaty people.

Table of Contents

List of Tables

List of Figures

Abstract

The current study investigates whether biochar and biochar-alginate composite (BAC), spiked with lead (Pb^{2+}), has the potential to be released into soil. The study assesses the sorption capacity and kinetics of Pb^{2+} between 5 to 94 mg L^{-1} in water using biochar & BAC as adsorbents; the portion of Pb^{2+} desorbed and released from the soil when spiked at 0, 10, and 100 mg L^{-1}; and the impact Pb^{2+} spiked adsorbents has on the microbial respiration of soil. Langmuir demonstrated a better fit for biochar and BAC with a maximum sorption capacity of 15.9 and 23.1 ug g^{-1}, respectively. A maximum of 1.85 and 1.15 ug L^{-1} of Pb^{2+} leached from the soil with spiked biochar and BAC, respectively, which remains below the acceptable Pb^{2+} limits in soil. Furthermore, non-spiked and Pb^{2+} spiked adsorbents, in the short-term, increases CO_2-C production when applied to soil. As time passes, microbial respiration decreases.

1.0 Introduction

Heavy metals are contaminants with densities greater than 5 g cm^{-3} such as cadmium, chromium, copper, lead, mercury, nickel, and zinc (Barakat, 2011). Sources of heavy metal wastes include petroleum refining, wood processing, metal plating, and printed circuit boards (Barakat, 2011; Renu et al., 2017). Heavy metals disrupt and cause serious health effects to humans, land and aquatic species, and different environments. For example, heavy metals are easily adsorbed by living organisms in aquatic environments due to their high solubility rates and may accumulate in the human body once they enter the food chain (Barakat, 2011). If the heavy metals ingested are greater than the maximum allowable concentration, serious health disorders may occur (Babel & Kurniawan, 2004).

Chemical precipitation, electrodialysis, ion exchange, oxidation, reduction, reverse osmosis, and ultrafiltration are types of heavy metal treatment technologies (Barakat, 2011; Renu et al., 2017). Each treatment technology demonstrates limitations such as inefficiencies, sensitive parameters, high-energy requirements, expensive operations, and toxic sludge production (Eccles, 1999; Renu et al., 2017). There is a demand for cost-effective and environmentally-friendly heavy metal removal methods such as absorbent materials which are effective and easy methods to safely remove heavy metals (Wang et al., 2019a).

Adsorption is the mass transfer of a substance that physically or chemically bounds the substance to a surface solid (Barakat, 2011). This concept may be applied to water treatment technology due to its easy operational use, wide range of adsorbents, and diverse removal while having the potential to remove biological, inorganic, insoluble, and

soluble contaminants (Ali, 2012). Heavy metal remediation commonly uses adsorbent materials and can easily and effectively remove heavy metals from contaminated water (Wang et al., 2019a). Therefore, adsorption is determined to be a method of treatment for removing heavy metals (Renu et al., 2017).

Several low-cost adsorbents have been produced from agricultural waste, industrial by-products, or natural materials and applied to metal contaminated media for the removal of heavy metals (Barakat, 2011). Biochar, derived from agricultural wastes, has the potential to be a source of low-cost adsorbents. Derived from wood, manures, agricultural residues, or leaves, biochar is a carbon (C) rich material obtained from thermal degradation when biomass is transitioned in a limited to zero oxygenated environment (Lehmann & Joseph, 2009). Traditionally, biochar is applied to soil improving fertility and increasing C sequestration in the hopes to mitigate climate change (Lehmann, 2007b). Soil fertility improvement is observed mainly by a pH increase in acid soils or increasing nutrient retention through cation adsorption (Liang et al., 2006; Van Zwieten et al., 2010). Therefore, when present in soil, biochar's contribution to the physical nature of the system can be significant. The composition of biochar, including phase, molecular, and surface structure, changes during the pyrolysis process which draws attention to the material as a treatment technology for heavy metals (Zheng et al., 2010) in contaminated wastewater and soil. Alone, biochar generally has low adsorption capacity (Fang et al., 2016) thus, improving the adsorption capability of biochar to expand environmental applications as treatment technology has developed into an important area of research (Ahmad et al., 2014; Rajapaksha et al., 2016; Wang et al., 2017). Alginic acid salt extracted from brown seaweeds (Lee & Mooney, 2012) has

researchers interested for use as a composite with biochar. Alginate beads serve as a stable matrix for types of absorbents that have fine particles (Wang et al., 2019b) and several studies have been conducted investigating the interactions between biochar and calcium-alginates. Together, a biochar-alginate composite (BAC) possesses a larger surface area than other composites and alginate have alone (Wang et al., 2018a). The BAC demonstrates superior adsorption capacity and is inexpensive compared to other heavy metal removal adsorbents (Do & Lee, 2013). For example, in an aqueous solution, the calculated adsorption costs measured in US \$0.950 ± 0.100 g^{-1} of Pb^{2+} for BAC (8:1 ratio), alginates, and active carbon were 0.250 ± 0.100, 0.830 ± 0.100, and 0.950 ± 0.100, respectively. Furthermore, the adsorption capacity of BAC was 78.0 % and 79.0 %, which were similar to alginates alone with values of 71.0 % and 82.0 % (Biswas et al., 2019; Wang et al., 2018a). Although using BAC is a method for treating contaminated water, contaminated BAC are being disposed into landfill. There is currently no available literature discussing end-of-life management practices for biochar and/or BAC used for remediation methods such as heavy metal removal. However, there are two studies investigating the consequences of disposing chemically treated wood for biochar and ash into soil. The studies focus on the environmental risk of applying contaminated biochar and wood ash to soil by assessing crop growth, metal bioavailability and soil microbial activity. Both studies found the availability of heavy metals to be significantly higher in contaminated wood ash soil treatments compared to contaminated biochar (Jones & Quilliam, 2014; Lucchini et al., 2014). Furthermore, the availability of As, Cd, Ni, and Pb to be lower in soils treated with heavy metal contaminated biochar versus non treated soil (Lucchini et al., 2014). There is potential to dispose of contaminated biochar and/or BAC

used in heavy metal water remediation in soil however, further studies are needed. The overall objective of the study is to determine the adsorption and desorption kinetics of Pb^{2+} when spiked directly on biochar and BAC and evaluate the sorption and desorption dynamics of Pb^{2+} spiked biochar and BAC in soil.

2.0 Literature Review

2.1 Biochar

2.1.1. Beneficial Use

Biochar is an organic treatment technology widely known for recovering soil fertility, and mitigating climate change by sequestering C (Lehmann, 2007b). Applying biochar to soil improves water-holding capacity, microbial respiration, and soil aeration, increases organic C, cation exchange capacity (CEC), decreases acidity in soil (Sohi et al., 2010), and increases plant micronutrient availability (Van Zwieten et al., 2010). Moreover, large quantities of organic functional groups in biochar interact with contaminants in soil; therefore, the immobilization and removal of heavy metals through sorption increases (Van Zwieten et al., 2010; Xu et al., 2014). The adsorption capability of biochar has lead researchers to further expand its environmental applications (Ahmad et al., 2014; Rajapaksha et al., 2016; Wang et al., 2017). Therefore, applying biochar to sediment and aqueous solutions (including industrial and municipal wastewater, surface and ground water) to improve aquatic ecosystems is a growing area of research.

2.1.2. Production & Application of Biochar

It is critical to understand the main elements of biochar production that control the physicochemical properties for the environment and society to benefit from biochar as a treatment technology (Sun et al., 2014). Through decades of research it has been determined heating temperature and feedstock were the fundamental elements that significantly impact the properties of biochar (Ronsse et al., 2013; Tag et al., 2016). The biomass available with different pyrolysis processes causes the variation in physicochemical properties of biochar. The different physicochemical properties of

biochar define its functions and applications (Ronsse et al., 2013). Therefore, both pyrolysis temperature and feedstock composition determine some of the characteristics biochar will possess such as CEC, porosity, surface area, biochar yield, acidity level, ash, and C content.

2.1.2.1. Heating Rate

The pyrolysis heating rate is the rate at which the biomass is thermally heated to form biochar. Heating rate is the combination of the highest thermal temperature (HTT) and the residence time. Heating rate defines the characteristics and by-products for biochar while the temperature defines surface properties and pore structure (Sohi et al., 2010), including surface area, C reactions, pH, volatile matter, CEC, and functional groups (Tomczyk et al., 2020).

2.1.2.1.1. Surface area

Surface area is a highly important characteristic controlling the adsorption capability of biochar for chemical compounds. Greater porous structures contribute to higher surface area (Inyang et al., 2010; Yao et al., 2011). Experimentally, a positive correlation between temperature and surface area has been demonstrated (Ronsse et al., 2013; Sun et al., 2014; Uchimiya et al., 2011b). As pyrolysis temperature increases, the surface area of feedstock also increases. Sorption of organic and inorganic contaminants are superior when biochar is produced at temperatures greater than 400 °C (Uchimiya et al., 2011b). The surface area increased from 12.9 to 401 m^2 g^{-1}, 13.6 to 388 m^2 g^{-1}, and 10.2 to 375 m^2 g^{-1} for hickory wood, bagasse, and bamboo biochar, respectively, from 450 to 600 °C (Sun et al., 2014). Hickory wood, bagasse, and bamboo biochar demonstrated surface area increases of 30 times its size when the pyrolysis temperature

increased from 450 to 600°C. Similar results were demonstrated by Ronsse et al., (2013) with a wood surface area of 196 m^2 g^{-1} at 600 °C with a residence time of 10 minutes. Therefore, biochar produced at 600 °C are perhaps more useful for water treatment or environmental remediation (Sun et al., 2014). In addition to increasing the temperature of biochar, the duration of pyrolysis also impacts surface area. Longer residence times show a reduction in surface area of 127 to 69 m^2 g^{-1} at identical pyrolysis temperatures when increased from 10 to 60 min (Ronsse et al., 2013).

2.1.2.1.2. pH

Biochar generally ranges from a weak acidic to alkaline with a pH value of 6.5 to 10.8 (Inyang et al., 2010; Lehmann et al., 2011; Tag et al., 2016; Yuan et al., 2011). The formation of carbonates and deconstruction of alkalis determine the pH value of biochar (Ding et al., 2014; Yuan et al., 2011). There is a positive correlation between pyrolysis temperature and pH value of biochar. The breakdown of alkali salts from organic materials increases causing the pH value to rise as the production temperature rises (Tag et al., 2016). Initially, near 200 to 300 °C, biochar produces acids and phenolics substances due to the decomposition of cellulose and hemicellulose. A lower intensity pyrolysis process retains a greater quantity of labile, oxygenated C (Ronsse et al., 2013). With greater pyrolysis temperature and residence time, the quantity of carboxyl and acidic groups present in biochar are reduced and deprotonated, respectively, causing pH values to increase (Ronsse et al., 2013; Tag et al., 2016). The pH level of biochar rises as more acidic groups are deprotonated to the conjugated base (Ronsse et al., 2013). The pH value increases as alkali salts begin separating above 300 °C from the organic matrix (Yu et al., 2014). At 600 °C, all alkali salts are released causing pH to become constant

(Shinogi & Kanri, 2003). Furthermore, increasing temperature and/or residence time increases the ash content present in biochar which causes the pH to become more alkaline (Ronsse et al., 2013). Tag et al., (2016) experimentally demonstrated that the extent pH levels will increase with pyrolysis temperature is dependent on the ash content present. Seaweed and poultry litter biochar had an average pH values of 12.0 and 10.7, respectively, with average ash contents of 33.5 and 18.3 %, respectively. In comparison, vine pruning and orange pomace biochar had smaller ash content values of 8.44 and 11.6 %, respectively, and lower pH values of 9.83 and 9.40, respectively. Therefore, greater ash content will cause the pH value to be higher as the temperature increases. In addition, a positive correlation of 0.960, 0.920, 0.940, and 0.940 between temperature and ash content was identified for vine pruning, orange pomace, seaweed, and poultry litter, respectively (Tag et al., 2016).

2.1.2.1.3. Cation Exchange Capacity

CEC demonstrates the magnitude that biochar can adsorb cationic nutrients (Tag et al., 2016) and research reveals the CEC of biochar decreases as pyrolysis temperature increases (Mukherjee et al., 2011; Song & Guo, 2012; Yao et al., 2012). Biochar contains aliphatic and cellulose type structures when processed at temperatures between 250 to 400 °C (Novak et al., 2009) whereas, higher temperature biochar (600 to 700 °C) contain well-organized C layers and are hydrophobic in their nature (Uchimiya et al., 2011a). The well-organized C layers display a graphene structure with less surface functional groups present and the removal of surface functional groups decrease CEC (Ahmad et al., 2014; Joseph et al., 2010). The nature and distribution of oxygenated functional groups on the surface of biochar effects the CEC of biochar (Banik et al., 2018) while the dehydration

and deoxygenation of feedstock lowers hydrogen and oxygenate functional groups (Ahmad et al., 2014; Uchimiya et al., 2011a). Larger quantities of oxygenated functional groups promotes a greater release of cations (Ahmad et al., 2014). Oxonium groups (heteroatoms in aromatic rings) possess the positive charge of the surface functional groups where the carboxylic and phenolic groups contribute to the negative surface charge sites (Banik et al., 2018).

2.1.2.2. Feedstock

Feedstock is another term for biomass that is thermally degraded to produce biochar (Verheijen et al., 2010). Any organic material can be used, including wood, manure, and leaves (Lehmann & Joseph, 2009). Generally, feedstock materials can also be derived from biowastes including sewage sludge, poultry manures, municipal waste, and compost (Verheijen et al., 2010). Feedstock type and composition are one of the most crucial factors controlling the characteristics of biochar (Verheijen et al., 2010). The behaviour and functions of feedstock is imitated in biochar because the structural composition of feedstock, both chemical and structural, share the structural composition of the evolved biochar (Verheijen et al., 2010).

2.1.2.2.1. Composition of Feedstock

The feedstock chosen for biochar affects biochar yields, ash content, and available nutrients. The key composition elements of feedstock are cellulose, hemicellulose, lignin, and ash contents (Verheijen et al., 2010). The content of cellulose and lignin present in feedstock determines how much of the feedstock composition remains during pyrolysis (Verheijen et al., 2010). Cellulose begins to decompose at temperatures under 50 °C and is characterized by decreasing polymerization degree. As pyrolysis temperature begins to

increase, aromatic C forms in biochar. A significant loss of mass occurs in the form of volatiles creating an amorphous C matrix as cellulose decomposes near 250 to 350 °C (Verheijen et al., 2010). Hemicellulose thermally degrades freely in comparison to cellulose. Hemicellulose begins decomposing at 100 °C whereas lignin decomposition range is 275 to 500 °C (Demirbas et al., 2004). Wood-based feedstocks produce resistant and coarser biochar with high C contents and mass yield compared to other agricultural waste biochar due to its lower hemicellulose and high lignin content (Chew & Doshi et al., 2011; Demirbas et al., 2004; Winsley et al., 2007). Higher lignin content increases the yield of biochar since lignin does not decompose as quickly as cellulose or hemicellulose (Demirbas et al., 2004; Tomczyk et al., 2020).

2.1.2.2.2. pH

As previously described, biochar generally ranges from a weak acid to alkaline with a pH value varying from 6.5 to 10.8 (Inyang et al., 2010; Lehmann et al., 2011; Tag et al., 2016; Yuan et al., 2011). Variations in pH values are a result of the feedstock type (Tomczyk et al., 2020). Wood-based feedstocks produce a biochar with a lower pH value compared to other feedstocks by two units (Ronsse et al., 2013; Tag et al., 2016). Elemental composition (including cellulose, hemicellulose, and lignin) and available oxygenated functional groups correlate with the pH value of biochar (Ronsse et al., 2013) and the oxygenated functional groups (including c-pyrone-type, chromene, diketone, and quinine) affect the alkalinity of biochar (Montes-Morán et al., 2004).

2.1.2.2.3. Surface Area & Ash Content

The decomposition of cellulose and hemicellulose, and the formation of channel structures of feedstock causes the surface area to increase during pyrolysis (Ahmad et al.,

2012). Furthermore, the decomposition of lignin increases the porosity of biochar (Chen et al., 2012). The release of volatile matter is dependent on the type of feedstock which in turn creates more pores (Shaaban et al., 2014). Ash content of feedstock negatively correlates with specific surface area in biochar (Ronsse et al., 2013). Mukome et al., (2014) experimentally supported available literature by determining wood-based biochar to possess the lowest ash content of 0.200 %, whereas green waste, straw, and algae biochar have ash contents of 3.50, 7.90, and 38.4 %, respectively. Furthermore, wood-based biochar has the greatest surface area of 127 m^2 g^{-1} compared to other biochar (Mukome et al., 2014) such as green waste, straw, and algae biochar which have potential surface areas of 46.0, 22.0, and 19.0 m^2 g^{-1}, respectively. Soft woods are more receptive to thermal degradation due to their composition, thus increasing the porosity in the wood structure; effectively increasing the surface area (Mukome et al., 2014). The non-combustible components of feedstock are also dependent on the type of feedstock which also influences the specific surface area (Wang et al., 2015). Demirbas et al., (2014) observed high ash content from grass, grain husks, manures, and straw residue versus wood-based feedstocks, whereas, Mukome et al., (2014) showed wood feedstocks of biochar have a lower ash content (<7 %) compared to non-wood feedstocks. Ash content of the feedstock type causes the variance of decreasing volatile matter and the increasing of fixed C content in biochar (Tag et al., 2016).

2.1.2.2.4. Cation Exchange Capacity

Cation exchange capacity of biochar is determined by the type of feedstock (Tomczyk et al., 2020) and establishes the magnitude of cation nutrients biochar can adsorb (Tag et al., 2016). Comparatively, non-wood-based biochar has a higher surface

acidity and CEC than wood-based biochar (Mukome et al., 2014). In two separate experiments, poultry litter biochar was demonstrated to have higher CECs of 38.3 and 48.4 cmol kg^{-1} compared to orange pomace, pine chips, and peanut hulls of 29.9, 5.00, and 4.60 cmol kg^{-1}, respectively. (Gaskin et al., 2008; Tag et al., 2016). The change in results could be caused by the reduction in oxygenated function groups present on the surface of biochar and/or the combination of carboxylic functional groups, which contribute most of the CEC among the acidic functional groups, and specific surface area (Carrier et al., 2012; Singh et al., 2010; Suliman et al., 2016).

2.2. Alginates

2.2.1. Biochar-Alginate Composites

It is difficult to apply and remove biochar from aqueous solutions due to the small particle sizes (Wang et al., 2018c). Fortunately, biochar is a material that can be absorbed by alginates to create an alginate-based composite. The calcium-alginate bead encapsulates the biochar by absorbing the fine particles into its gel structure but allows liquids to pass through. The stable matrix structure successfully increases the function of biochar in aqueous solutions.

2.2.1.1. Adsorption

Alginate is utilized for the encapsulation of biological and chemical compounds in numerous applications due to its ability to create crosslinks with cations, biocompatibility, nontoxicity (Wang et al., 2019b), and reusability (Gotoh et al., 2004). Sodium alginate undergoes a crosslink reaction when a divalent cation is added. The divalent cation is exchanged with sodium from specific acid blocks (such as glucuronic which is a common building block of proteoglycans and glycoglycerolipids) which forms

an insoluble-water gel (Wang et al., 2019b). For example, adding Ca^{2+} with sodium alginates displaces part of H^{+} and Na^{+} to create a calcium-alginate gel (Wang et al., 2019b). Thus, alginate beads function as a stable matrix for types of absorbent that have fine particles and are hard to remove from aqueous solutions (Wang et al., 2019b). Absorbents include active C and biochar which have difficulties separating and/or regenerating from effluent since they are fine powders and result in significant loss of the adsorbent.

Adsorption of Cd^{2+} by an *Ambrosia trifida* biochar-alginate bead was studied using batch systems and continuous fixed bed columns. This combination successfully determined that the biochar-alginate could be an adsorbent for the removal of Cd^{2+} from groundwaters (Roh et al., 2015; Wang et al., 2018a). In a comparative study, Do & Lee (2013) observed the adsorption of Pb^{2+} significantly improved in an aqueous solution with calcium-alginate crosslinked with biochar compared to using biochar alone. Using the Langmuir adsorption model, the BAC and pinewood biochar maximum adsorption capacities were 263 and 0.900 mg g^{-1}, respectively. Bamboo biochar, BAC, and calcium-alginate maximum adsorption capacities for Cd^{2+} were 40.0, 227, and 252 mg g^{-1}, respectively (Wang et al., 2018a). The increase in adsorption was due to the high adsorption capacity of the calcium-alginate. Also, the synergetic interaction between biochar and calcium-alginate exposes active sorption sites for biochar and calcium-alginate. Moreover, the lower cost of biochar renders the BAC to be more cost-effective compared to calcium-alginates in large scale applications (Wang et al., 2018a).

2.2.1.2. Biochar-Alginate Ratio

In the available research, there is not extensive research about the mass ratio of biochar and alginates. There are variations in biochar-alginate mass ratios in available studies however, no optimal conditions are suggested. A study constructed a mass ratio of 1:3 bamboo biochar and calcium-alginate resulting in a 5.60 % decrease in adsorption capacity from the calcium-alginate relative to the BAC (Wang et al., 2018b). A higher percentage of calcium-alginate was used to test the hypothesis that calcium-alginates will improve the stabilization of biochar (Wang et al., 2018b). Another study fabricated a 8:1 mass ratio of biochar to calcium-alginate resulting in the BAC having a 50 % Pb^{2+} loss of adsorption capacity relative to the alginate gel (Do & Lee, 2013); however, the adsorption capacity of the BAC continued to be greater than biochar alone to remove Pb^{2+}. Compared to other types of biochar, the BAC removed 132 to 261 mg g^{-1} more of Pb^{2+} (Do & Lee, 2013). A ratio of 4:1 bamboo biochar to calcium-alginate was used in a different study resulting in a 9.80 % loss of Cd^{2+} adsorption capacity in the BAC relative to a calcium-alginate gel (Wang et al., 2018). While different studies have tested different percentages of biochar compared to calcium-alginate in order to decrease costs, other reasonings for the specific ratio implemented are not discussed.

2.2.1.3. Desorption

Alginates are alginic acids and as an adsorbent they can use acids such as HCl, HNO_3, and H_2SO for regeneration (Biswas et al., 2019; Do & Lee, 2013). The type and amount of acid is influenced by the type of heavy metal desorption. There are not many available studies demonstrating desorption capacity or reusability of BAC. Due to the gap in research there was a vast variation between the two available studies. The first study

observed a constant desorption of Pb^{2+} of approximately 90.0 % through 10 consecutive cycles (Do & Lee, 2013), whereas the second study observed a decrease in the regeneration capacity after each cycle when the BAC was reused (Biswas et al., 2019). Desorption of Zn^{2+} demonstrated a recyclability of 85.0, 73.0, 35.0 and 29.0 % after the first, second, third and fourth cycle, respectively (Biswas et al., 2019). There was a 56.0 % change in desorption capacity after four cycles. The difference between the two studies was in the decrease in concentration of acid applied to the BAC. Do & Lee (2013) demonstrated experimentally that desorption efficiency will increase as the acid concentration also increases up to a certain threshold. Therefore, it can be shown that a 0.15 mol L^{-1} increase could be due to the ion exchange between the heavy metal and H^{+}. Further research needs to be conducted to not only support this theory but demonstrate additional desorption capacity results.

2.2.1.4. Pb^{2+} Spiked Biochar & BAC Amendment in Soil

There is currently no available literature discussing the impacts of Pb^{2+} in soil when applied with spiked biochar and BAC after remediating contaminated waters. Over the past couple decades, wood ash produced from wood mills has been applied to soil not only as a soil amendment but, more importantly, to reduce the amount of ash in landfills (Pugliese et al., 2014). Field soil samples were conducted with the addition of ash subsamples and were mixed thoroughly (Pugliese et al., 2014). The change in soil pH, ash pH, soil nutrients, heavy metals, and soil microbial activity were analyzed in the process (Hannam et al., 2018; Pugliese et al., 2014; Zimmermann & Frey, 2002). In short-term studies, ash demonstrated positive effects on soil in regard to pH, nutrients, and heavy metals, and no significant effects on the microbial biomass and activity

(Pugliese et al., 2014; Zimmermann & Frey, 2002). Similarly, two other studies investigated the environmental risk of applying contaminated biochar and wood ash by assessing crop growth, metal bioavailability and soil microbial activity. Both studies determined a decrease in the availability of heavy metals found in soil mixed with contaminated biochar versus contaminated wood ash (Jones & Quilliam, 2014; Lucchini et al., 2014). As, Cd, Ni, and Pb demonstrates higher bioavailability in non-treated soil versus soil mixed with biochar derived from contaminated wood waste (Lucchini et al., 2014). Furthermore, Jones & Quilliam (2014) conclude low levels of contamination from Cu-treated wood should pose minimal environmental risk to biochar and ash destined for land application.

3. Research Objectives & Hypotheses

3.1. Research Objectives

The research was completed in two studies: 1) a sorption-desorption capacity and kinetic study and 2) a biochar, BAC, and soil amendment study. Study one focuses on determining both the adsorption and desorption capacities and kinetics of biochar and BAC and determining the physical and chemical structure of adsorbents. Study two evaluates desorption and transport of Pb^{2+} from spiked biochar and BAC in soil columns and determines the effect of Pb^{2+} spiked biochar & BAC have on soil microbial activity. Therefore, the research objectives are:

1. Determine adsorption and desorption capacities and kinetics of Pb^{2+} in water using biochar or BAC as adsorbents
2. Determine the proportion of Pb^{2+} that is desorbed from biochar or BAC and released into the soil in a leaching column
3. Evaluate the impact of Pb^{2+} spiked biochar or BAC in soil on microbial respiration by measuring CO_2 evolution

3.2. Research Hypotheses

The hypotheses are as follows:

1. Concentration of Pb^{2+} has a positive correlation with biochar & BAC adsorbing Pb^{2+}
2. BAC will have superior adsorption capacity
3. Treatments more likely to desorb Pb^{2+} will have higher amount of Pb^{2+} leach from the soil
4. Soils amended with Pb^{2+} spiked BAC will have greater microbial respiration

5. As Pb^{2+} concentration increases, Pb^{2+} will inhibit carbon release when soils are amended with Pb^{2+} spiked biochar & BAC

4. Sorption Capacity & Kinetics of Pb^{2+} Spiked Biochar & BAC

4.1. Introduction

Decades of research has determined heating temperature and feedstock the fundamental elements that impact the properties of biochar (Ronsse et al., 2013; Tag et al., 2016). As previously mentioned, the heating rate and temperature of biochar defines the by-products, surface properties and pore structure (Sohi et al., 2010); where the feedstock defines the biochar yields, ash content, and available nutrients (Verheijen et al., 2010). Heating temperature and feedstock are specifically chosen for the application type of biochar to maximize its treatment. In the current study, biochar was used for water remediation of heavy metals. Biochar composed of birch wood was chosen due to its large surface area for adsorption and was produced at 400 °C to further promote sorption of organic and inorganic contaminants (Ronsse et al., 2013; Sun et al., 2014; Uchimiya et al., 2011b). At 400 °C, cellulose, hemicellulose and lignin of the wood feedstock decomposes and increases surface area and porosity of biochar (Ahmad et al., 2012; Chen et al., 2012). Some wood types, including birch, are receptive to thermal degradation and increasing the porosity in the wood structure; effectively increasing the surface area (Mukome et al., 2014).

The encapsulation of biochar using alginates was an alternative option for water remediation of heavy metals. As previously mentioned, it was difficult to apply and remove biochar from aqueous solutions due to the small particle sizes (Wang et al., 2018c). Alginate beads function as a stable matrix which undergoes a crosslink reaction when a divalent cation such as $CaCl_2$ is added. Research demonstrates the divalent cation was exchanged with sodium from specific acid blocks (such as glucuronic which is a

common building block of proteoglycans and glycoglycerolipids) which forms an insoluble-water gel (Wang et al., 2019b). The beginning of the current study focuses on combing birch biochar with sodium alginate to form a biochar-alginate composite (BAC) beads. The physical structure and chemical properties of biochar and BAC were analyzed to determine their adsorption characteristics including pH, CEC, and surface area. Furthermore, the preparation and formation of biochar and (BAC) were investigated to maximize both biochar and BAC adsorption and desorption capacities in removing and holding lead (Pb^{2+}), respectively. Defining the best preparation and formation of both adsorbents in controlled conditions will help understand the amount of Pb^{2+} that could potentially be desorbed based on the amount of Pb^{2+} spiked and adsorbed in both adsorbents. Therefore, to fully understand the amount of Pb^{2+} that could be released into soil when spiked Pb^{2+} biochar and BAC are mixed into soil, it was crucial to understand both the adsorption and desorption dynamics of the adsorbents; therefore, the current chapter focuses on the how the characterization and form of biochar and alginates impacts sorption dynamics and assesses the use of alginates. The current adsorption and desorption experimental designs were created incorporating experimental parameters used in Biswas et al., (2019), Do & Lee (2013), and Liu et al., (2020) to determine the sorption quantity of Pb^{2+} with biochar and BAC. Since the maximum acceptable concentration (MAC) of Pb in Nova Scotia drinking water is 5 $\mu g\ L^{-1}$ (Health Canada, 2019), and it has been estimated that 10 % (19,740) of private Nova Scotian wells exceed the threshold where many have concentrations of Pb greater than 10 $\mu g\ L^{-1}$ (Health Canada, 2020; Sweeney et al., 2017). Therefore, a Pb^{2+} concentration range of 5 to 100 $\mu g\ L^{-1}$ was the focus for spiking biochar and BAC.

In the first study, scanning electron microscopy (SEM) and energy dispersive spectroscopy (EDS) system determined the surface morphology and chemical structure, respectively; and sorption experiments were conducted to determine the adsorption and desorption capacities and kinetics of spiked Pb^{2+} biochar and BAC. Langmuir isotherm to estimate the maximum sorption capacity and both isotherms to evaluate the type of Pb^{2+} adsorption and desorption occurring. It was hypothesized that the concentration of Pb^{2+} has a positive correlation with biochar & BAC adsorbing Pb^{2+} and BAC will have greater adsorption capacity than biochar alone.

4.2. Materials & Methods

4.2.1. Chemical Reagents

Calcium chloride ($CaCl_2$, 96% of purity) and sodium alginate were purchased from Acros Organics - Fisher Scientific Co. (Ottawa, ON, Canada) where the sodium alginate was extracted from brown algae in powder form and was not further purified. Nitric acid (HNO_3, ≥98% of purity), sodium hydroxide (NaOH, ≥97% of purity), and Pb^{2+} (SPEXertificate, 1000 ug mL^{-1}) were also purchased from Fisher Scientific Co. (Ottawa, ON, Canada).

4.2.2. Biochar Preparation

Birch biochar was given by the Department of Chemistry at Cape Breton University (Sydney, NS, Canada) which was provided by B. W. Bioenergy Inc. The birch biochar was prepared by pyrolysis of debarked birch wood at approximately 400 °C for 30 min followed by rapid quenching in cold water (Carrier et al., 2017). The biochar received was further grounded and sieved to 53 μm particle size. Birch biochar was used for both biochar and biochar-alginate composite (BAC).

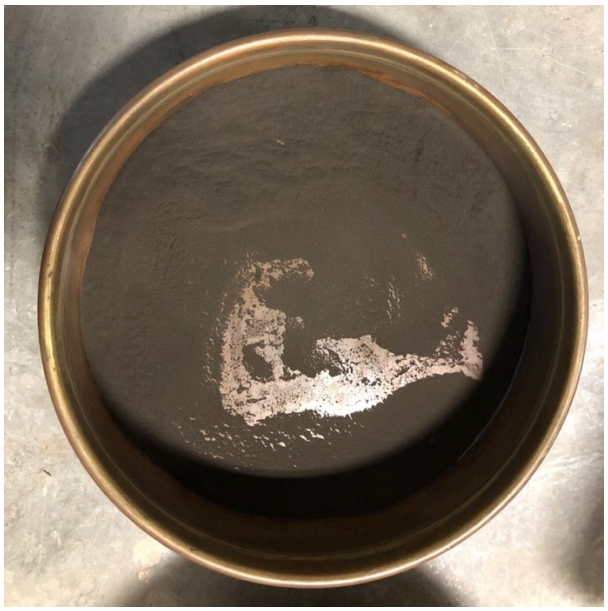

Figure 1. Sieving birch biochar to 53 μm.

4.2.3. Biochar-Alginate Composite Bead Preparation

Biochar-alginate composite (BAC) beads were created using the 4:1 ratio of birch biochar and sodium alginates. A solution containing 4 % (w/v) of biochar, 1 % (w/v) of alginate were mixed with deionized water using magnetic stirrer for 30 mins at 70 °C. Using a modified method provided by Do & Lee (2013) and Biswas et al., (2019), the mixed solution was slowly poured into a 50 mL volumetric burette. Droplets of the mixture fell from the volumetric burette into 0.27 M $CaCl_2$ room temperature solution on a magnetic stirrer at 60 rpm. Biochar and alginate formed a spherical membrane immediately when the composite came into contact with $CaCl_2$ solution where biochar was immobilized inside the membrane. BAC beads remained mixing on the magnetic stirrer in $CaCl_2$ solution to harden for 30 min.

Figure 2. 4 % (w/v) of biochar and 1 % (w/v) of alginate weighed prior to adding to deionized water and mixing on the magnetic stirrer.

Figure 3. Biochar-alginate composite (BAC) droplets forming in $CaCl_2$ creating a bead.

Afterwards, the beads were washed multiple times to ensure all excessive biochar and/or $CaCl_2$ were removed. BAC was stored in deionized water in the refrigerator at 2 °C for the adsorption-desorption and soil amendment experiments.

Figure 4. Biochar-alginate composite (BAC) between deionized water rinsing stages.

4.2.4. Characterization of Biochar & BAC

Elemental analysis and textural properties of birch biochar were determined previously by Carrier et al. (2017). The surface morphology of dried biochar and BAC were identified using scanning electron microscopy (SEM) and elemental analysis of BAC was determined using an Oxford Inca energy dispersive spectroscopy (EDS) system. The surface area of biochar was identified using the Brunauer-Emmett-Teller (BET) method and moisture content was calculated by the difference between the weight before and after being dried for 24 h in a dry oven at 60 °C. Bulk density was calculated by the mass of dry sample divided by the total volume used.

4.2.5. Adsorption Experiment

Biochar and BAC were prepared as described in sections 4.2.2 and 4.2.3. Stock solutions of Pb^{2+} (1000 μg mL^{-1}) were prepared by dissolving Pb^{2+} with deionized water creating desired Pb^{2+} solutions of 5, 10, 25, 50, 75, and 100 μg L^{-1}. The actual Pb^{2+} stock solutions created were slightly different from the desired Pb^{2+} stock solutions with concentrations of 5, 12, 28, 50, 62, and 94 μg L^{-1}. In total, 72 experimental units were completed including the triplication of each experimental unit. The adsorption experiment included the following Pb^{2+} spiked treatments: 1) 5; 2) 12; 3) 28; 4) 50; 5) 62;

and 6) 94 μg L^{-1}. The final treatment was the control group: 7) 0 μg L^{-1} which was biochar and BAC mixed with deionized water. Biochar and BAC experimental units had a dry weight of 0.05 g mixed with 50 mL Pb^{2+} spiked solutions. The pH of each experimental units were adjusted to 5.0 ± 0.2 with the addition of HNO_3 and NaOH.

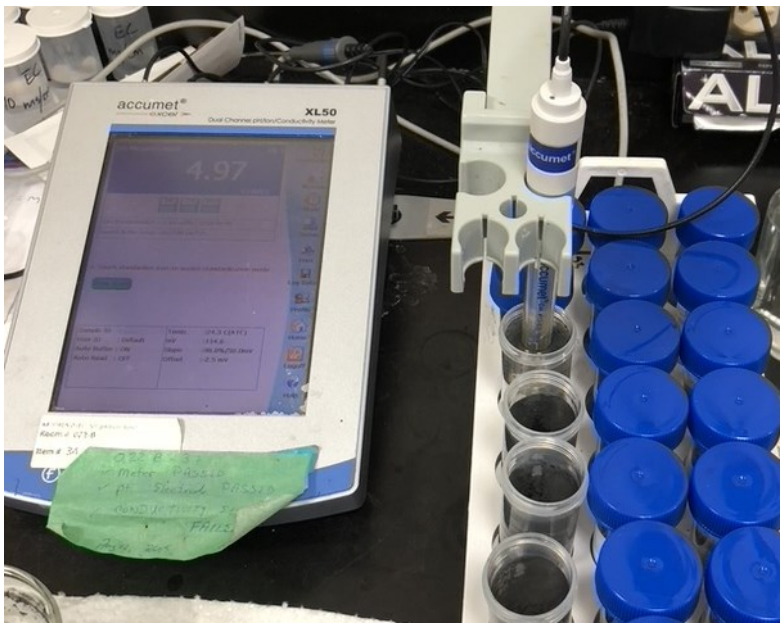

Figure 5. Adjusting the pH of biochar and BAC solutions with Pb^{2+} to 5 using HNO_3 and NaOH.

All experimental units were shaken horizontally at 60 rpm at room temperature (20 °C) using a benchtop Eberbach Corporation Shaker (115 volts, 07047 A5407WVS, Van Buren Charter Township, MI, United States). The experimental units were placed randomly to create a Completely Randomized Design (CRD). Biochar experimental units were shaken: 1) 3; and 2) 7 days with Pb^{2+} spiked treatments which were represented as B3 and B7, respectively. Two treatments were measured since previous research was unable to confirm when biochar reached Pb^{2+} adsorption equilibrium (Carrier et al. 2017). All BAC experimental units were shaken for 1 day with spiked Pb^{2+} which were

represented as BAC. Available research found the majority of BAC adsorbed Pb^{2+} within 2 h and reached full equilibrium after 24 h (Do & Lee, 2013; Liu et al., 2020; Wang et al., 2018a). After shaking, 50 mL biochar experimental units were centrifuged with International Centrifuge Tachometer from International Equipment Co. (Boston, MA, United States). A trial and error process determined the 2 h centrifuge time of the 50 mL biochar experimental units. BAC experimental units were filtered with Q2 Quantitative filter papers from Fisher Scientific Co. (Ottawa, ON, Canada) to separate adsorbents from the aqueous solution. All aqueous Pb^{2+} spiked solutions were acidified with HNO_3 to 1 % (v/v) and stored in refrigerators at 2 °C until they were ready to be analyzed.

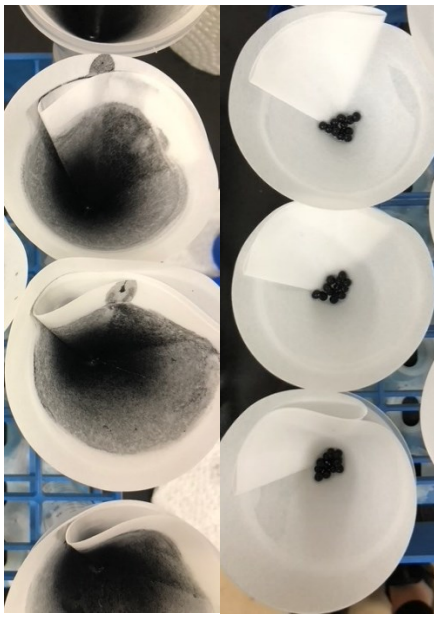

Figure 6. Centrifuging and filtering biochar and BAC, respectively, after adsorption.

4.2.6. Desorption Experiment

After separating the adsorbents from the aqueous solutions, biochar experimental units were washed with deionized water and dried in the oven overnight at 60 °C. BAC experimental units were also washed with deionized water and filtered with Q2

Quantitative filter paper. All the experimental units remained separated during the transition from adsorption to desorption experiment.

Since previous research was unable to determine Pb^{2+} sorption equilibrium using biochar, Pb^{2+} spiked biochar experimental units were shaken: 1) 3; and 2) 7 days in the desorption experiment which were represented as 1) B3D3 (biochar 3-day adsorption and desorption); 2) B3D7 (biochar 3-day adsorption and 7-day desorption); 3) B7D3 (biochar 7-day adsorption and 3-day desorption); 4) B7D7 (biochar 7-day adsorption and desorption). Since BAC reached full equilibrium in 24 h (Do & Lee, 2013; Liu et al., 2020; Wang et al., 2018a), Pb^{2+} spiked BAC experimental units were shaken for 1 day. Desorption concentrations of Pb^{2+} spiked biochar and BAC were: 1) 5; 2) 12; 3) 28; 4) 50; 5) 62; and 6) 94 $\mu g\ L^{-1}$. In total, 120 biochar and BAC experimental units were conducted including the triplication of each experimental unit using an approximate dry weight of 0.05 g. Very small amounts of biochar remained in the 50 mL tubes when transitioned into weighing tins and oven drying due to the fine particles.

Figure 7. Transitioning biochar after oven drying into 50 mL tubes for desorption experiment.

The pH value of each experimental unit was adjusted to 5.0 ± 0.2 with the addition of HNO_3 and NaOH. Biochar and BAC were shaken horizontally with the benchtop Eberbach Corporation Shaker. The experimental units were placed randomly in the shaker to create a CRD. Both adsorbents were shaken with 50 mL of 0.2 M HNO_3 to desorb Pb^{2+} from the adsorbents. The final treatment was the control group: 7) 0 μg L^{-1} which was biochar and BAC mixed with deionized water. Similar to the adsorption process, after shaking, 50 mL biochar experimental units were centrifuged for 2 h with International Centrifuge Tachometer. BAC experimental units were filtered with Q2 Quantitative filter papers to separate adsorbents from the aqueous solution. All aqueous solutions were acidified with HNO_3 to 1 % (v/v) and stored in refrigerators at 2 °C until they were ready to be analyzed.

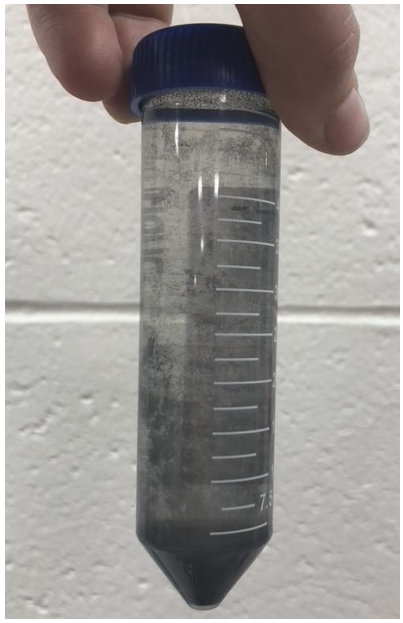

Figure 8. Post 2 h centrifuged 50 mL tubes with biochar and HNO_3 solution after shaking to desorb Pb^{2+}.

4.2.7. Data Analysis

Sorption experimental units were analyzed using an Agilent 7800 ICP-MS (1500 W RF power, 10 mm sample depth, 206, 207, 208 isotopes, internal Bi standard) in the Department of Chemistry at the University of Acadia (Wolfville, NS, Canada). Pb^{2+} was measured as the sum of isotopes 206, 207, and 208, and Bi-209 was used as an internal standard). QA/QC protocol incorporated a certified reference material (simulated natural water: CRM-TMDW-A, High-Purity Standards) which was traceable to the NIST 3100 series, reagent blanks, and continuing calibration verification to assess method accuracy. Recoveries were typically within ±10 % of the accepted value. In addition, a duplicate soil sample to monitor analytical precision and a method blank to measure background was analyzed once every ten samples. All experimental units were completed in triplicate at room temperature and the average experimental data was used. Surface morphology was measured using SEM. The amount of spiked Pb^{2+} adsorbed and desorbed by biochar and BAC were calculated by measuring the initial and final concentrations of Pb^{2+}. Adsorption and desorption isotherm models including Langmuir and Freundlich were determined using the following non-linear and linear models:

$$Langmuir\ original\ model:\ q_e = \frac{q_m b C_e}{1+bC_e} \quad (1)$$

$$Langmuir\ linear\ model:\ \frac{1}{q_e} = \frac{1}{q_m} + \frac{1}{q_{mK_L}}\frac{1}{C_e} \quad (2)$$

$$Freundlich\ original\ model:\ q_e = kC_e^{\frac{1}{n}} \quad (3)$$

$$Freundlich\ linear\ model:\ logq_e = logk + \frac{1}{n}\ logC_e \quad (4)$$

where q_e (μg g^{-1}) was the Pb^{2+} adsorbed at equilibrium; q_m (μg g^{-1}) was the maximum adsorption capacity; C_e (μg L^{-1}) was the equilibrium concentration in the solution; b (L

μg^{-1}) and k ($(\mu g\ g^{-1})(L\ \mu g^{-1})^{1/n}$) were the adsorption equilibrium constants for Langmuir and Freundlich models, respectively. 1/n measured the adsorption intensity or surface heterogeneity and as the value becomes closer to 0, the surface becomes more heterogeneous (Haghseresht & Lu, 1998).

Furthermore, Langmuir model can also be explained by a dimensionless constant separation factor, R_L, (Hall et al., 1966), which indicates the feasibility of adsorption process for various initial Pb^{2+} concentrations (Biswas et al., 2019). The separation factor was defined by:

$$R = \frac{1}{1+bC_i} \quad (5)$$

where b was the Langmuir constant (L mg^{-1}); C_i was the initial concentration (mg L^{-1}). The R value indicates if the isotherm is favourable (0<R<1), unfavorable (R>1), or irreversible (R=0) (Do & Lee, 2013).

4.2.8. Statistical Analysis

Regressions were calculated for both Langmuir and Fruendlich isotherms by plotting the inverse of the equilibrium concentration in the solution (C_e) and Pb^{2+} adsorbed at equilibrium (q_e) on the x- and y-axis, respectively, using Microsoft Excel. A trendline was added for each treatment to determine the regression equation and coefficient. Standard deviation between triplicates and confidence levels were determined using Minitab® Statistical Software Web App. Repeated measure analysis of variance, ANOVA, was applied since the responses from the experimental units measured repeated over the length of the experiments. Three factors of interest that were used in the repeated measure of ANONVA included sorption time (1, 3, and 7 days), adsorbent material (biochar and BAC), and Pb concentration (0, 5, 12, 28, 50, 62, and 94 μg L^{-1}). A CRD

was used and the data compliance was determined using the Anderson-Darling Normality test. If the assumption of normality and constant variance were verified ($\rho \geq 0.1$) a comparison by Fisher's Least Significant Difference test would be completed to calculate the difference between means at a significance level of $\alpha = 0.05$. However, if the assumption of normality and constant variance were violated ($\rho \leq 0.1$), data transformations were conducted on the response variables. Furthermore, if the treatments significantly impacted the sorption capacity ($\rho \leq 0.05$), means of the triplicate experimental units were compared with the Least Square Means test.

4.3 Results

4.3.1. Characterization of Biochar & BAC

Elemental analysis of birch biochar and BAC were completed and the pH of biochar and BAC were found to be slightly alkaline and almost neutral, respectively (Table 1). The surface area of biochar was found to be 259 $m^2\ g^{-1}$. Other textural properties include micropore surface area, micropore volume, and average pore width of 198 $m^2\ g^{-1}$, 0.105 $cm^3\ g^{-1}$, and 23.2 Å, respectively (Carrier et al., 2017). Moisture content of biochar and BAC were 4.20 ± 0.100 and 90.0 ± 0.200 %, respectively, and the bulk density was 0.0906 and 0.879 g cm^{-3}, respectively. The surface morphology of dried biochar were identified and shown in Figure 9 and Figure 10, respectively. The birch biochar morphology retains the visible wood capillaries and those particles demonstrate an irregular nonuniform size distribution (Carrier et al., 2017). The macropores enables diffusion of adsorbates throughout the particles where the distribution becomes limited as the particles reach the micropores inside the capillary walls (Carrier et al., 2017). The wet weight of a single BAC was approximately 0.0238 g and has a diameter of 3.00 ± 0.200

mm. The addition of alginates stabilizes biochar particles (Figure 10a) and has a smoother surface (Figure 10b) compared to biochar alone (Figure 9).

Table 1. Element composition, pH, moisture content (MC), bulk density, and initial Pb^{2+} amount of biochar and biochar-alginate composite beads (BAC) prior to spiking.

Adsorbent	**C (%)**	**O (%)**	**N (%)**	**H (%)**	**Ca (%)**	**S (%)**	**Ash (%)**	**pH**	**MC (%)**	**Bulk Density (g cm^{-3})**	**Initial Pb^{2+} concen-trations (µg L^{-1})**
Biochar	87	-	0.3	2.6	-	0.10	>0.10	7.4	4.2 ± 0.10	0.091	3.19 ± 0.20
BAC	63	26	8.1	-	3.5	-	-	6.8	90 ± 0.20	0.88	1.51 ± 0.04

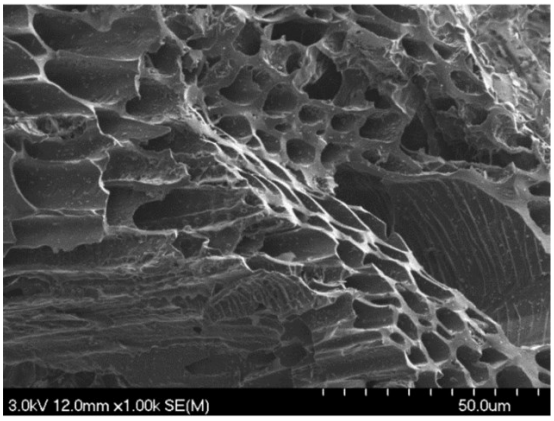

Figure 9. SEM image of the birch biochar after pyrolysis (Carrier et al., 2017).

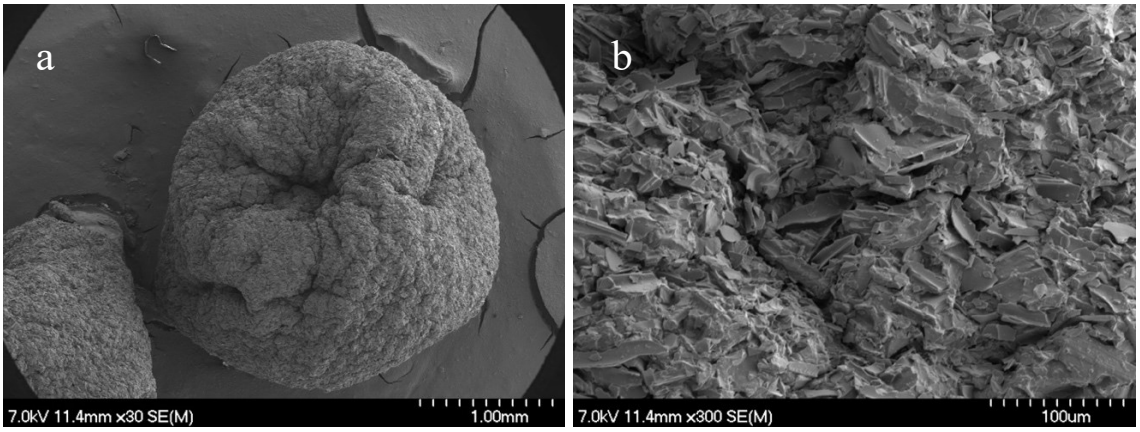

Figure 10. Image of BAC at x30 SEM (a) and image of BAC at x300 SEM (b).

4.3.2. Adsorption-Desorption Capacities

To determine if the majority of biochar reached equilibrium after the third day or if 7 days was needed, both time periods were recorded and demonstrated in Table 2. B3 treatment had the greatest difference from B7 and BAC treatments with the lowest adsorption capacity with an average adsorption value of 80.5 %. Whereas, B7 and BAC treatments showed almost identical results for each experimental unit with an average adsorption capacity of 94.6 and 94.2 %, respectively. Although B3 treatment demonstrated the lowest adsorption capability for most Pb^{2+} concentrations, each adsorbent treatment demonstrated similar adsorption capacities for each Pb^{2+} concentration. Furthermore, the various spiked Pb^{2+} concentrations significantly impacted the adsorption capacity for each adsorbent treatment. Excluding 5 $\mu g\ L^{-1}$, Pb^{2+} concentrations were directly proportional to the adsorption capability of biochar and BAC. The concentration of Pb^{2+} demonstrated a positive correlation with biochar & BAC adsorbing Pb^{2+} therefore, as Pb^{2+} concentration increased in the spiked adsorbetns, the adsorption capacity of Pb^{2+} with biochar and BAC also increased. Biochar and BAC at 62 and 94 $\mu g\ L^{-1}$ Pb^{2+} concentrations demonstrated almost identical adsorption capacities in

the experiment. However, both biochar and BAC adsorption abilities peaked at 62 μg L^{-1}. Biochar and BAC had the lowest adsorption capacity at Pb concentration of 12 and 5 μg L^{-1}, respectively.

Table 2. Adsorption of the various biochar and BAC treatments at each Pb^{2+} concentration (n=3).

Pb^{2+} concentration (μg L^{-1})	Adsorption Capacity (%) Treatment		
	[1]B3	[2]B7	[3]BAC
5	87.6 [4]C[5]b ± 0.01	94.0 Ca ± 0.00	82.4 Ca ± 0.05
12	51.5 Db ± 0.04	86.4 Da ± 0.04	93.8 Da ± 0.03
28	66.1 Eb ± 0.11	94.1 Ea ± 0.02	94.6 Ea ± 0.04
50	87.3 Bb ± 0.01	95.9 Ba ± 0.01	98.3 Ba ± 0.00
62	95.8 Ab ± 0.01	99.0 Aa ± 0.01	98.8 Aa ± 0.00
94	94.5 Ab ± 0.01	97.9 Aa ± 0.01	97.3 Aa ± 0.00

[1]B3 biochar with an adsorption time of 3 days
[2]B7 biochar with an adsorption time of 7 days
[3]BAC biochar-alginate composite with an adsorption time of 1 day
[4] The capital letters represent significant differences ($p<0.05$) within the column (concentrations)
[5] The lower-cased letters represent significant differences ($p<0.05$) across rows (adsorption time)

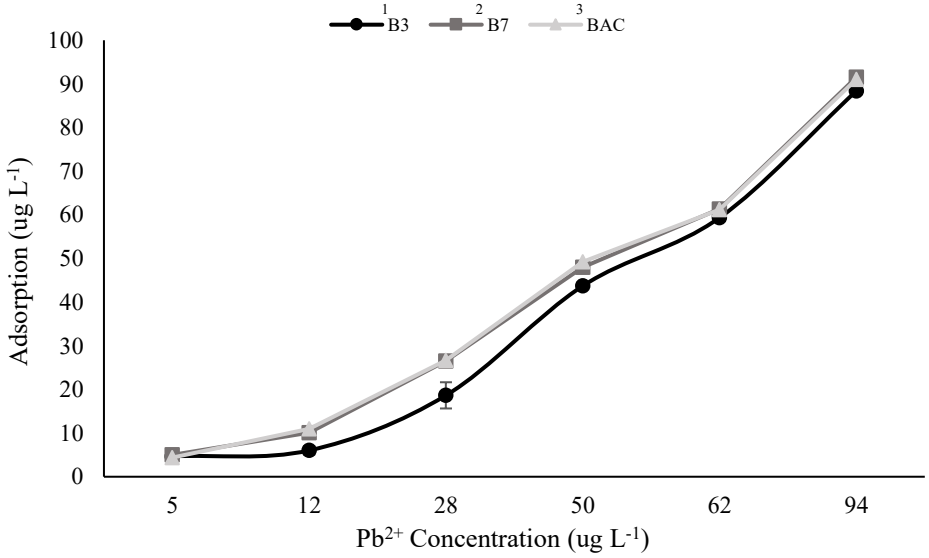

[1]B3 biochar with an adsorption time of 3 days
[2]B7 biochar with an adsorption time of 7 days
[3]BAC biochar-alginate composite with an adsorption time of 1 day

Figure 11. Adsorption capacities of B3D3, B3D7, B7D3, B7D7, and BAC treatments at each Pb^{2+} concentration (n=3).

The methods were carried over to the desorption experiment and considered 3 and 7 day desorption contact time for both B3 and B7 adsorption treatments. Both time periods were recorded and demonstrated in Table 3. BAC had a significantly higher desorption capacity than each biochar treatment. Unlike the adsorption experiment, biochar and BAC had variances in their desorption capacities. B3D7 and B7D7 treatments demonstrated similar results in their experimental units whereas, B7D3 treatment demonstrated the lowest desorption capacity in the experiment. Similar to adsorption experiment, the largest Pb^{2+} concentration demonstrated one of the greatest desorption abilities and each adsorbent treatment demonstrated similar adsorption capacities for each Pb^{2+} concentration. B7D3, B7D7, and BAC had the greatest desorption capacity at Pb^{2+}concentration of 94 μg L^{-1} whereas B3D3 and B3D7 treatments had the greatest desorption capacity at 5 μg L^{-1}. Not as evident as in the adsorption experiment, the desorption of biochar and BAC had a systematic increase but at overall lower values.

The control samples were not included in either Table 2 or Table 3, however, Pb^{2+} was found to be present in the control experimental units in both adsorption and desorption experiments. The control adsorption experimental units left minimal traces of Pb^{2+} with values ranging between 0.07-0.44 μg L^{-1}. The control desorption experimental units had concentrations of Pb^{2+} with values as high as 3.97 μg L^{-1} which was close to the MAC provided by Health Canada.

Table 3. Desorption of the various biochar and BAC treatments at each Pb^{2+} concentration (n=3).

Pb^{2+} concentration ($\mu g\ L^{-1}$)	Desorption Capacity (%) Treatment				
	[1]B3D3	[2]B3D7	[3]B7D3	[4]B7D7	[5]BACD
5	81.9 [6]B[7]b ± 0.12	72.2 Ac ± 0.03	51.2 Cd ± 0.03	63.7 Bc ± 0.06	69.6 BCa ± 0.08
12	86.3 Ab ± 0.05	78.0 Ac ± 0.07	71.5 ABd ± 0.05	80.7 Ac ± 0.02	88.5 Aa ± 0.04
28	77.3 Bb ± 0.00	69.7 ABc ± 0.06	46.8Dd ± 0.11	67.8 Bc ± 0.09	88.8 Aa ± 0.04
50	58.4 Cb ± 0.01	54.9 Cc ± 0.03	60.3BCd ± 0.09	59.0 Bc ± 0.00	65.1 Ca ± 0.03
62	59.4 Cb ± 0.03	61.4 BCc ± 0.05	60.9BCd ± 0.02	56.4 Bc ± 0.14	73.0 Ba ± 0.01
94	75.2 Bb ± 0.04	69.2 ABc ± 0.06	78.6Ad ± 0.07	83.1 Ac ± 0.01	92.2 Aa ± 0.03

[1]B3D3 biochar with an adsorption and desorption time of 3 days
[2]B3D3 biochar with an adsorption and desorption time of 3 and 7 days, respectively
[3]B7D3 biochar with an adsorption and desorption time of 7 and 3 days, respectively
[4]B7D7 biochar with an adsorption and desorption time of 7 days
[5]BACD biochar-alginate composite with an adsorption and desorption time of 1 day
[6] The capital letters represent significant differences ($p<0.05$) within the column (concentrations)
[7] The lower-cased letters represent significant differences ($p<0.05$) across rows (adsorption time)

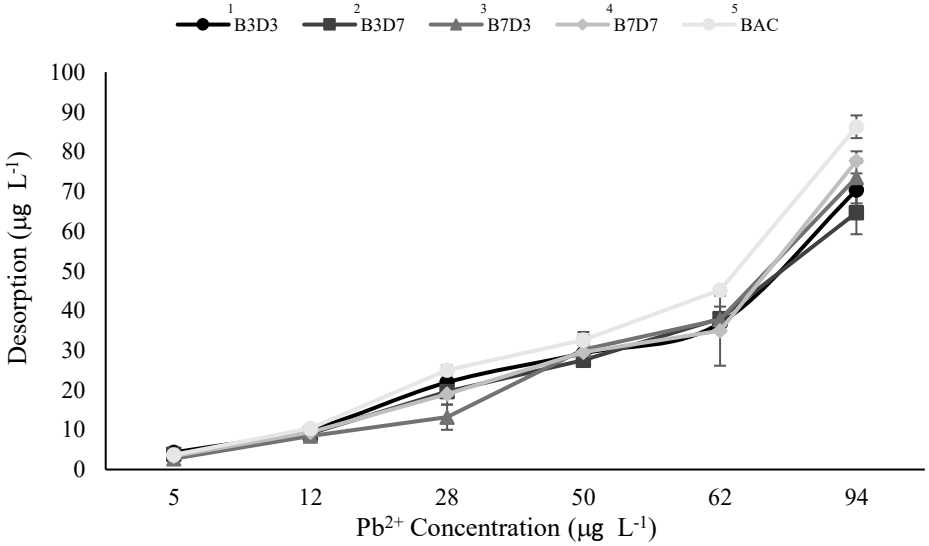

[1]B3D3 biochar with an adsorption and desorption time of 3 days
[2]B3D3 biochar with an adsorption and desorption time of 3 and 7 days, respectively
[3]B7D3 biochar with an adsorption and desorption time of 7 and 3 days, respectively
[4]B7D7 biochar with an adsorption and desorption time of 7 days
[5]BACD biochar-alginate composite with an adsorption and desorption time of 1 day

Figure 12. Desorption capacities of B3D3, B3D7, B7D3, B7D7, and BAC treatments at each Pb^{2+} concentration (n=3).

4.3.3. Sorption Isotherms

Common adsorption isotherms applied in water treatment applications to describe adsorption equilibrium are Langmuir and Freundlich isotherms (Liu et al., 2020). Langmuir and Freundlich isotherms were used to determine the interaction of adsorption and desorption by measuring the fitness of experimental data and Langmuir isotherm was also used to estimate the maximum sorption capacity. Langmuir isotherm was a monolayer adsorption model and explains the adsorption phenomenon on the homogeneous surface of the adsorbent (Langmuir, 1918). The adsorption on the surface was definite and localized and each site can accommodate only one adsorbent species (Do, 1998; Yang, 1987). Langmuir can predict an adsorbent's maximum adsorption capacity at a particular condition for a range of initial concentrations (Biswas et al., 2019; Osmari et al., 2013). Whereas Freundlich isotherm was a multilayer adsorption model. Freundlich explains the adsorption phenomenon on the heterogenous surface of the adsorbent (Biswas et al., 2019) and provides exponential distribution of active sites and energy at the sites (Ayawei et al., 2017). Langmuir and Freundlich isotherms for biochar and BAC adsorption were calculated and demonstrated in Figure 13 and Figure 14, respectively. Implementing a linear regression formula for each treatment, the slope, intercept, and regression coefficient (R^2) were calculated and R^2 values were shown in Table 4. Langmuir isotherm fits the experimental data better for both biochar and BAC (R^2 in the range of 0.802-0.930; Figure 13) however, BAC experimental units fits the Freundlich model as well ($R^2 = 0.810$; Figure 14). The higher R^2 value suggests biochar and BAC interacted with Pb^{2+} as a homogenous surface along the monolayer adsorption (Wang et al., 2018a) however, BAC also had multilayer Pb^{2+} adsorption occur. Biochar

and BAC demonstrate high surface area which favours monolayer adsorption on the adsorbent surfaces (Do & Lee, 2013; Ho et al., 2002).

The linearity parameter, n, suggests a more homogenous surface for BAC compared to biochar. As previously mentioned, the birch biochar morphology retained the visible wood capillaries and those particles demonstrate an irregular nonuniform size distribution (Carrier et al., 2017) causing variation in the surface area. The SEM images of biochar and BAC in Figure 9 and Figure 10a, respectively, support Carrier et al., (2017) assertion that nonuniform wood capillaries cause variation in the surface whereas, BAC thoroughly mixed together biochar and alginates with a magnetic stirrer for 30 mins at 70 °C and placed into $CaCl_2$ to form a uniform membrane over the biochar. Moreover, the linearity parameter indicated a non-linear sorption since biochar and BAC were between 0.5 and 1.1 (Zhang et al., 2017). The linear regression for the treatments for both Langmuir and Freundlich in Figure 13 and Figure 14, respectively, do not follow a linear sorption line due to the variation in the amount of Pb^{2+} adsorbed at the different Pb^{2+} concentrations.

The maximum adsorption capacity from Langmuir isotherm was calculated using the slope of each treatment and Langmuir constant (K_L) and Freundlich constant (K_f) were calculated using the intercepts from the isotherms in Figure 13 and Figure 14, respectively. Langmuir maximum adsorption capacity of Pb^{2+} for B3, B7, and BAC were 7.03, 16.0, and 23.1 $\mu g\ g^{-1}$ respectively. BAC maximum adsorption capacity was greater than biochar however, B3 had less variability than BAC with Langmuir isotherm. Moreover, the separation factor, R_L, in Figure 15 of Langmuir isotherm was calculated to determine the feasibility at various Pb^{2+} concentrations. There was a decrease in R_L with

increasing Pb^{2+} concentrations for both adsorbents. All R_L values of adsorption were between 0 and 1 at all concentrations for biochar and BAC and confirms favourable adsorption of Pb^{2+}.

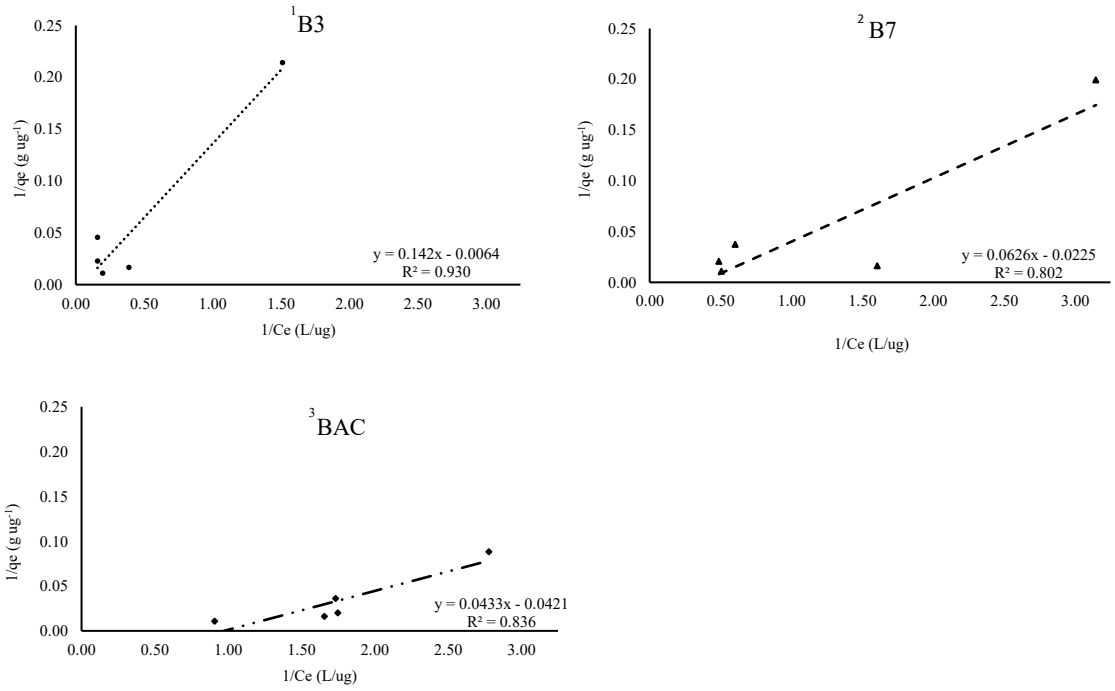

[1]B3 biochar with an adsorption time of 3 days
[2]B7 biochar with an adsorption time of 7 days
[3]BAC biochar-alginate composite with an adsorption time of 1 day

Figure 13. Langmuir adsorption isotherm of Pb^{2+} absorbed onto B3, B7, and BAC in the adsorption experiment (n=3).

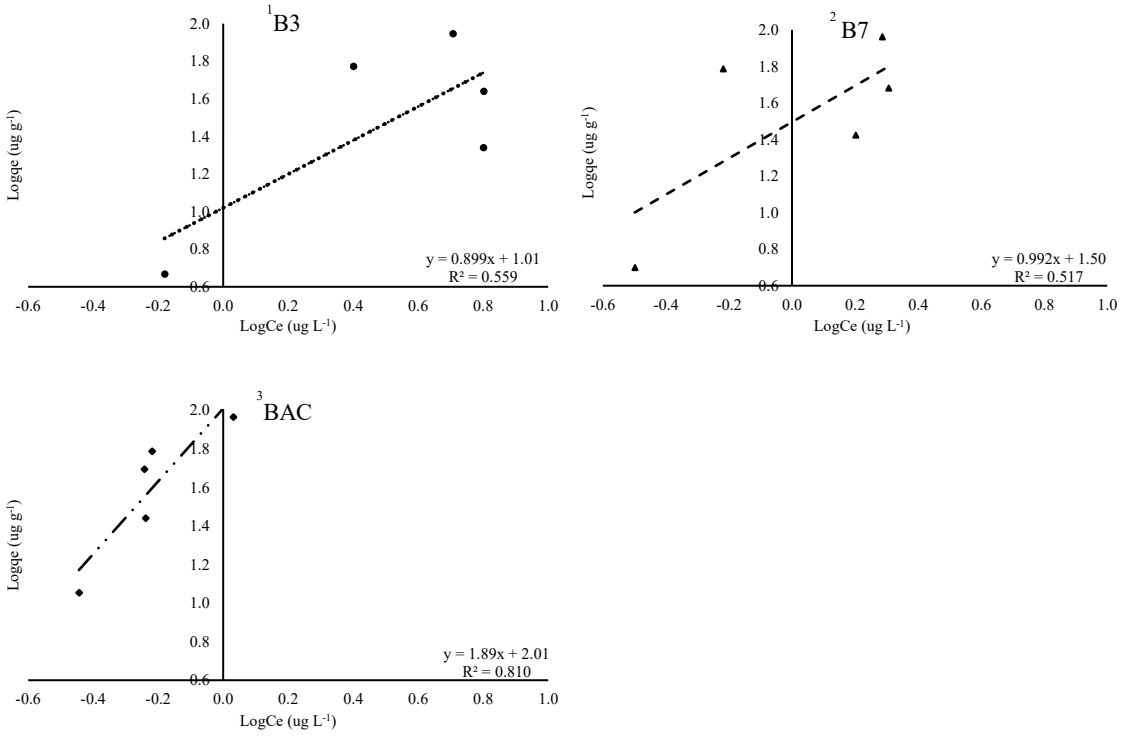

[1]B3 biochar with an adsorption time of 3 days
[2]B7 biochar with an adsorption time of 7 days
[3]BAC biochar-alginate composite with an adsorption time of 1 day

Figure 14. Freundlich adsorption isotherm of Pb^{2+} absorbed onto B3, B7, and BAC in the adsorption experiment (n=3).

Table 4. Adsorption constants for Langmuir and Freundlich isotherms and regression coefficient from calculated linear regression formula for B3, B7, and BAC treatments (n=3).

	Langmuir constants			Freundlich constants		
Treatment	[1]q_m	[2]K_L	[3]R	[4]K_f	[5]1/n	[3]R
B3	7.03	-22.2	0.930	10.5	0.899	0.559
B7	16.00	-2.78	0.802	31.3	0.992	0.517
BAC	23.1	-1.03	0.836	102	1.89	0.810

[1]Maximum adsorption capacity ($\mu g\ g^{-1}$)
[2]Langmuir constant ($L\ \mu g^{-1}$)
[3]Regression coefficient
[4]Freundlich constant ($\mu g\ g^{-1}$)($L\ \mu g^{-1}$)$^{1/n}$
[5]Linearity parameter

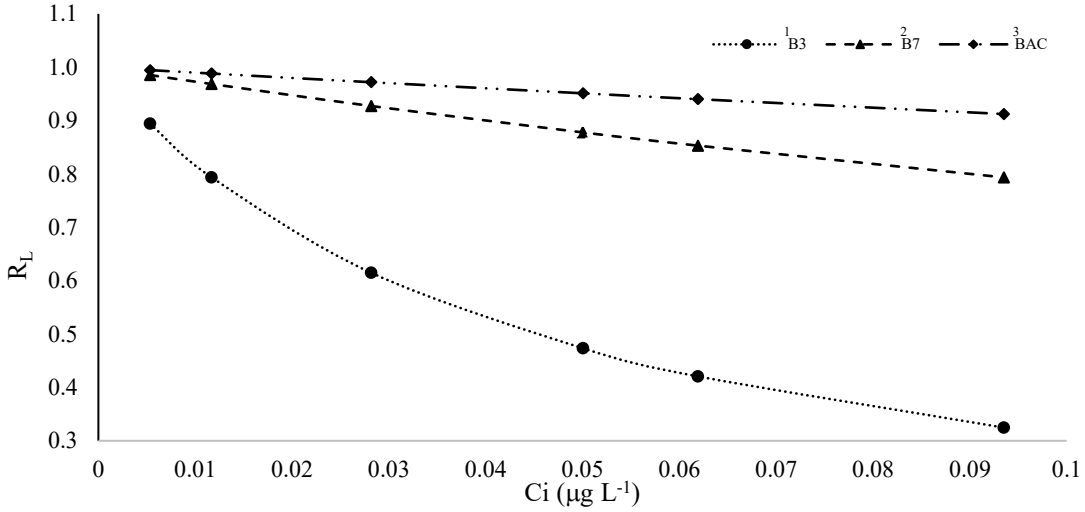

[1]B3 biochar with an adsorption time of 3 days
[2]B7 biochar with an adsorption time of 7 days
[3]BAC biochar-alginate composite with an adsorption time of 1 day

Figure 15. Separation factor, R_L, which indicates the feasibility of adsorption process for various initial Pb^{2+} concentrations (Biswas et al., 2019) for Langmuir adsorption isotherm for B3, B7, and BAC treatments (n=3).

Identical procedures were followed to measure the desorption capacity of biochar and BAC with Langmuir model (Figure 16) and Freundlich model (Figure 17). Implementing a linear regression formula for each treatment, the slope, intercept, and regression coefficient (R^2) were calculated and R^2 values were shown in Table 5. Langmuir isotherm fits best for B3D3 and B3D7 treatments, Freundlich isotherm fits best for B7D3, and BAC treatments, and both isotherms fit B7D7 treatment. Biochar treatment B3D7 had the greatest fit with Langmuir model with a R^2 value of 0.963 which suggests biochar interacted with Pb^{2+} as a homogenous surface with monolayer desorption (Wang et al., 2018a). Whereas, BAC had a higher R^2 value for Freundlich indicating multilayer desorption (Wang et al., 2018d). The linearity parameter indicated a more homogenous surface for BAC and biochar treatments with longer adsorption and desorption time. Similar to adsorption, the linearity parameter indicated a non-linear desorption since biochar and BAC were between 0.50 and 1.10 (Zhang et al., 2017)

which supports the variation in the amount of Pb^{2+} desorbed at the different Pb^{2+} concentrations of treatments for Langmuir (Figure 16) and Freundlich (Figure 17). The maximum desorption capacity from Langmuir isotherm was calculated using the slope of each treatment and Langmuir constant (K_L) and Freundlich constant (K_f) were calculated using the intercepts. Langmuir maximum desorption capacity of Pb^{2+} for all treatments were demonstrated in Table 5 where biochar treatment B3D3 had the greatest desorption capacity followed by BAC with values of 5.01 and 4.51 $\mu g\ g^{-1}$, respectively. Overall, there was more variability in the desorption experiment and no trend in biochar and BAC desorption capacity was seen. Moreover, the separation factor, R_L, in Figure 18 of Langmuir isotherm was calculated to determine the feasibility at various Pb^{2+} concentrations. There was a decrease in R_L with increasing Pb^{2+} concentrations for all adsorbents. All R_L values of desorption were between 0 and 1 at all Pb^{2+} concentrations for biochar and BAC which confirms favourable desorption of Pb^{2+}.

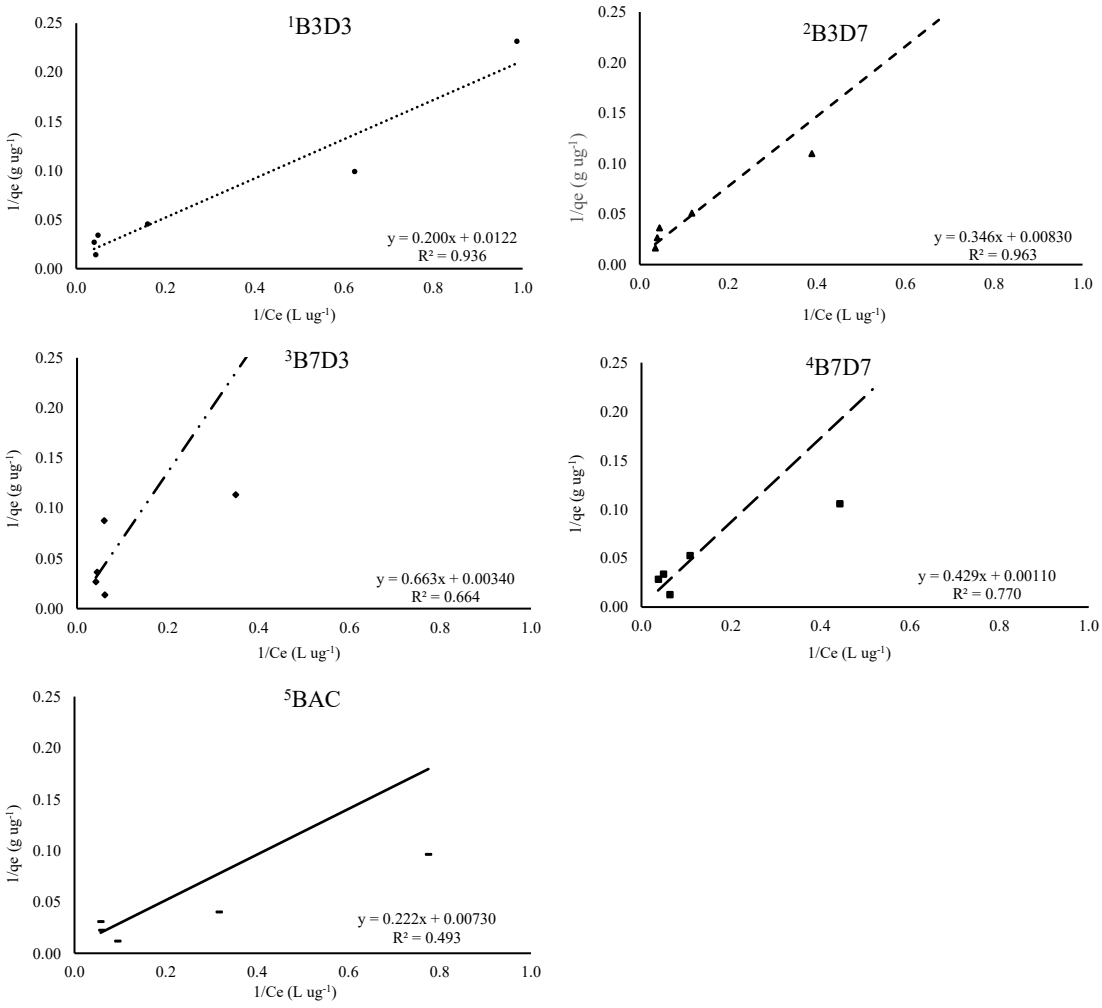

[1]B3D3 biochar with an adsorption and desorption time of 3 days
[2]B3D3 biochar with an adsorption and desorption time of 3 and 7 days, respectively
[3]B7D3 biochar with an adsorption and desorption time of 7 and 3 days, respectively
[4]B7D7 biochar with an adsorption and desorption time of 7 days
[5]BACD biochar-alginate composite with an adsorption and desorption time of 1 day

Figure 16. Langmuir isotherm of desorbed Pb^{2+} from B3D3, B3D7, B7D3, B7D7, and BAC treatments in the desorption experiment (n=3).

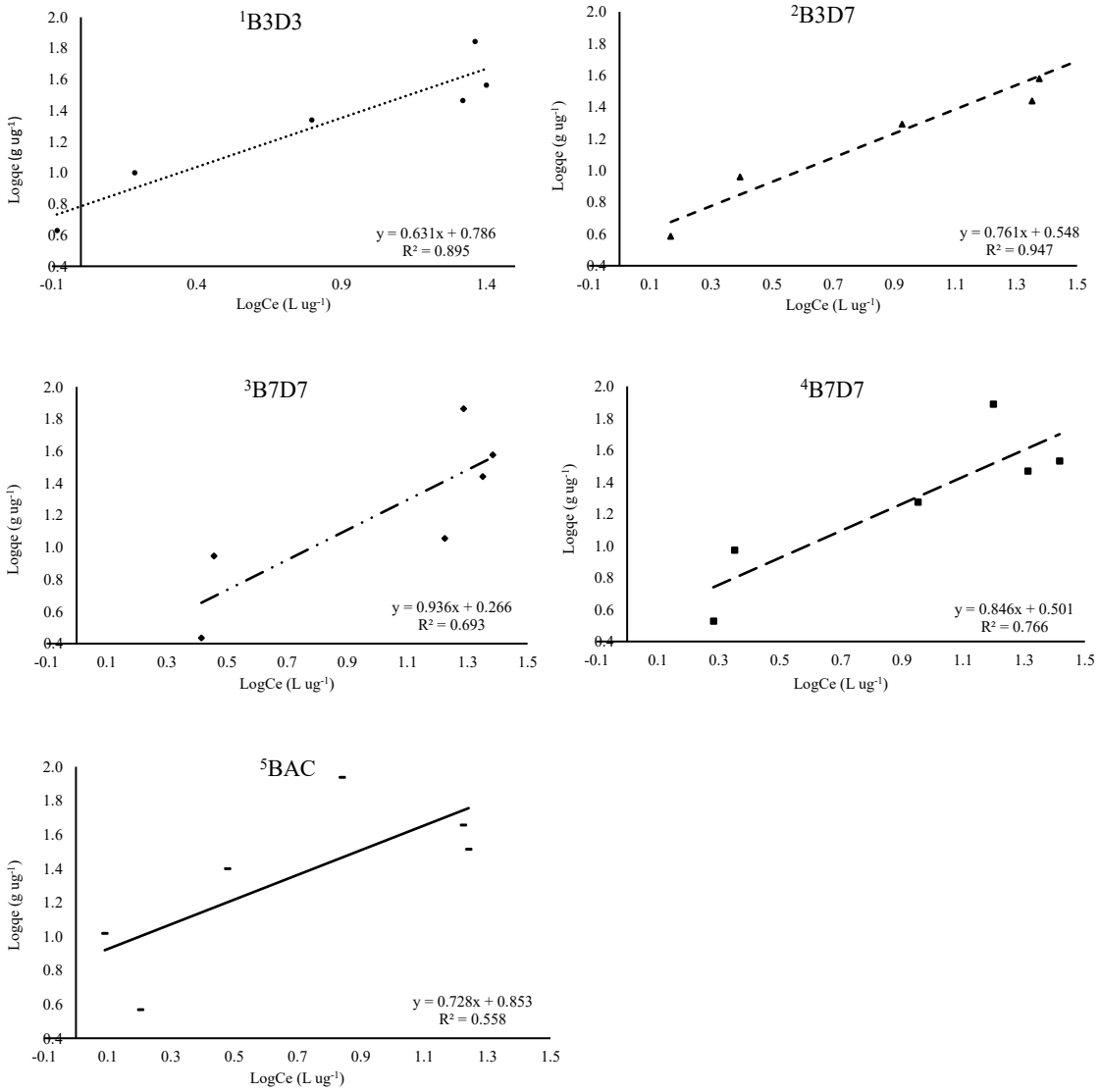

[1]B3D3 biochar with an adsorption and desorption time of 3 days
[2]B3D3 biochar with an adsorption and desorption time of 3 and 7 days, respectively
[3]B7D3 biochar with an adsorption and desorption time of 7 and 3 days, respectively
[4]B7D7 biochar with an adsorption and desorption time of 7 days
[5]BACD biochar-alginate composite with an adsorption and desorption time of 1 day

Figure 17. Freundlich isotherm of desorbed Pb^{2+} from B3D3, B3D7, B7D3, B7D7, and BAC treatments in the desorption experiment (n=3).

Table 5. Desorption constants for Langmuir and Freundlich isotherms and regression coefficient from calculated linear regression formula for B3, B7, and BAC treatments (n=3).

	Langmuir constants			Freundlich constants		
Treatment	[1]q_m	[2]K_L	[3]R	[4]K_f	[5]1/n	[3]R
B3D3	5.01	16.4	0.936	6.10	0.631	0.895
B7D3	2.88	44.5	0.963	3.49	0.777	0.947
B7D3	1.51	195	0.664	1.85	0.936	0.693
B7D7	2.33	390	0.770	3.17	0.846	0.766
BAC	4.51	30.4	0.493	7.13	0.728	0.558

[1]Maximum adsorption capacity (μg g^{-1})
[2]Langmuir constant (L μg^{-1})
[3]Regression coefficient
[4]Freundlich constant (μg g^{-1})(L μg^{-1})$^{1/n}$
[5]Linearity parameter

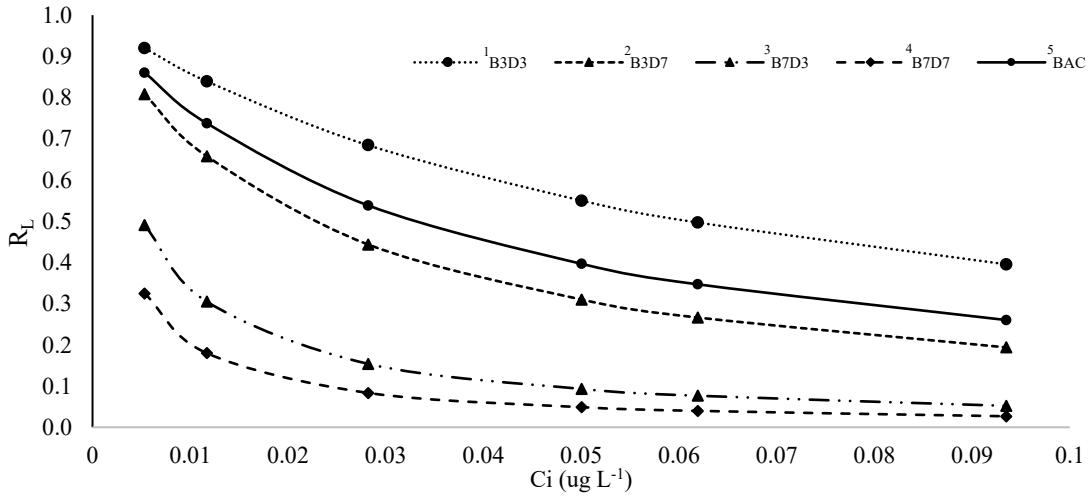

[1]B3D3 biochar with an adsorption and desorption time of 3 days
[2]B3D3 biochar with an adsorption and desorption time of 3 and 7 days, respectively
[3]B7D3 biochar with an adsorption and desorption time of 7 and 3 days, respectively
[4]B7D7 biochar with an adsorption and desorption time of 7 days
[5]BACD biochar-alginate composite with an adsorption and desorption time of 1 day

Figure 18. Separation factor, RL, which indicates the feasibility of desorption process for various initial Pb^{2+} concentrations (Biswas et al., 2019) for Langmuir adsorption isotherm for B3D3, B3D7, B7D3, B7D7, and BAC treatments (n=3).

4.4. Discussion

4.4.1. Sorption of Pb^{2+} to Biochar and BAC

The SEM images of birch biochar exhibited wood capillaries with an irregular nonuniform size with a smooth surface. The adsorption average pore width of the wood capillaries were found to be 23.0 Å (Figure 9). The dried BAC (Figure 10a) shows the irregular morphology of the beads. The addition of alginates encapsulates the biochar and provides a smooth barrier over the wood capillaries (Figure 10b). Using the BET method, the surface area of biochar was found to be 259 m^2 g^{-1} which is similar to biochar composed of pine needles with a surface area of 236 m^2 g^{-1} (Chen et al., 2008). Furthermore, birch biochar demonstrated greater surface area than other hardwood-based biochar which had the greatest surface area of 127 m^2 g^{-1} (Mukome et al., 2014). Surface area was a highly important characteristic controlling the adsorption capability of biochar for chemical compounds. The decomposition of cellulose and hemicellulose, and the formation of channel structures of feedstock causes the surface area to increase during pyrolysis (Ahmad et al., 2012) and overall a greater porous material. Therefore, in the current study, biochar and BAC increased the amount of Pb^{2+} being adsorbed due to their larger surface area and greater porosity (Table 2). Another important characteristic that impacts the adsorption of Pb^{2+} to biochar and BAC was the initial pH value. pH has the ability to impact the surface charge of an adsorbent, the degree of ionization of the adsorbate molecules, and the extent of dissociation of the functional groups on the active sites of the adsorbent (Nandi et al., 2009). The initial pH level of biochar and BAC in these experiments were 7.5 and 6.8, respectively. A pH level of 5.0 had been determined to be the optimum level for adsorption for several heavy metals including Pb (Do & Lee,

2013; Issabayeva et al., 2006; Liu & Zhang, 2009; Wang et al., 2018a). The change in the surface charge of biochar and alginates caused a decrease in adsorption at lower and higher pH levels. A lower pH had a higher chance of adsorbing H^+ onto biochar and BAC surface with the increase of H^+ available which decreases the accessibility of Pb^{2+} ions to the adsorbent surface. For example, Do & Lee (2013), found Pb adsorption capacity to be 127, 131, 134, and 132 mg g^{-1} at pH levels of 3.0, 4.0, 5.0, and 5.5, respectively, concluding the optimum Pb adsorption capacity at a pH level of 5.0. Furthermore, a similar study that focused on the adsorption of Cd^{2+} with ball-milled biochar in Ca-alginate beads concluded biochar and alginates to be rich in surface functional groups (Wang et al., 2018a). Together, the acid functional groups of biochar and alginates which are on the surface and molecule chain, respectively, could be altered by the protonation and deprotonation of carboxyl groups (Wang et al., 2018a). The adsorption of heavy metals can be based on the interactions between the metal contaminant and acidic oxygen-containing functional groups (Inyang et al., 2016). Therefore, at low pH (<4), heavy metal adsorption was low due to the competition between H^+ and metal ions for available adsorption sites (Wang et al., 2018a).

Two factors in the adsorption experiment that impacted the treatments were: 1) Time; and 2) Concentration. First, the two biochar treatments, B3 and B7, were measured to determine when biochar reached adsorption equilibrium. Table 2 demonstrates variances between treatment B3 and B7. An increase in adsorption from B3 to B7 treatment supports Carrier et al., (2017) data in which birch biochar reaches full adsorption in seven days. The lower adsorption capacity of B3 could be caused by cation exchanges still occurring between the H^+ and Pb^{2+} (Do & Lee, 2013). Second, excluding

Pb^{2+} concentration of 5 μg L^{-1}, Pb^{2+} concentrations had a positive correlation with biochar and BAC adsorbing Pb^{2+}. The lower Pb^{2+} concentrations demonstrate a lower adsorption capacity for all treatments whereas biochar and BAC adsorbed Pb^{2+} faster at greater concentrations for all treatments. Biswas et al., (2019), Liu et., (2020), and Wang et al., (2018a) identified the same trend with biochar and/or BAC. The adsorption site available per unit mass of adsorbent was permanent regardless of the total adsorbent mass. Therefore, having a larger adsorbent mass or increasing the adsorbent mass over a given spiked contaminate volume would likely decrease the availability of available active sites and specific surface area (Biswas et al., 2019; Wang et al., 2018a).

The objective of the desorption experiment was to determine the maximum amount of Pb^{2+} that could be released from the biochar and BAC. A concentration of 0.200 M of HNO_3 has been determined to be the optimal concentration for desorbing Pb^{2+} from biochar and BAC (Do & Lee, 2013; Gedam & Dongre, 2019) which was used in this desorption experiment (section 4.2.6.). Unlike the adsorption experiments, no trend was found in Pb^{2+} desorption capacity of biochar and BAC. The desorption capacity was not as high as Do & Lee (2013) and Gedam & Dongre (2019), which had values of 93.0 and 92.0 %, respectively. Both studies mention an increase in the desorption capacity of biochar and BAC with an increase of HNO_3 between 0.150 to 0.200 M due to the high presence of H^+ from HNO_3. Furthermore, two desorption studies mention the different pH levels changed the desorption capacity but do not further discuss why (Gedam & Dongre, 2019; Zama et al., 2017). In this desorption experiment, the same concentration of HNO_3 was used therefore, the decrease seen in desorption may be caused by the change in pH levels to 5.0. Wang et al., (2018d) and Zama et al., (2017)

investigated the desorption of Pb^{2+} from biochar with pH levels ranging from 3.5 to 9.5 and found that pH and desorption capacity were proportional. As the pH level rose, the amount of Pb^{2+} desorbed from biochar also increased. The increase of H^{+} available at a lower pH would decrease the accessibility of Pb^{2+} ions to the BAC surface (Do & Lee, 2013). Similar to adsorption, pH can impact surface charge of biochar and BAC which changes the degree of ionization and dissociation of the functional groups (Nandi et al., 2009). As previously mentioned, a pH level of 5.0 had been determined to be the optimum level for adsorption for several heavy metals including Pb (Do & Lee, 2013; Issabayeva et al., 2006; Liu & Zhang, 2009; Wang et al., 2018a). The change in the surface charge of biochar and alginates prior to shaking the spiked adsorbents with HNO_3 solution may have caused the decrease in desorption capacities for the adsorbents. Neither Do & Lee (2013) and Gedam & Dongre (2019) changed the pH of the spiked biochar and BAC prior to desorbing Pb^{2+} and both studies have a greater desorption capacity. Changing the pH level prior to desorbing or having a pH of 5.0 may not be optimal for desorption depending on the objective. Thus, pH of the desorption experiment would depend on how much Pb^{2+} was of interest to desorb.

4.4.2. Comparing Biochar and BAC

Biochar and BAC adsorbents were considered in the first study to assess the novelty of using alginates and determine whether a biochar-alginate composite had value. Previous studies have considered biochar-alginate ratios of 8:1 (Do & Lee, 2013), 4:1 (Biswas et al., 2019), 1:3 (Wang et al., 2018b), and 1:0.25 (Wang et al., 2018a). Alginates are costly compared to biochar and using a larger amount of alginates would increase the adsorption of BAC but would also increase the overall production cost. Two

experiments had a maximum adsorption of 263 and 227 mg g^{-1} using a biochar-alginate ratio of 8:1 and 1:0.25, respectively (Do & Lee, 2013; Wang et al., 2018a). Doubling the amount of alginates only increased the adsorption by 13 %. Furthermore, an adsorption experiment using a mass ratio of 1:3 and 4:1 bamboo biochar with alginates resulted in a 5.60 and 9.80 % decrease, respectively, in adsorption (Wang et al., 2018a; Wang, et al., 2018b). A formula considering product cost, specifically alginates versus adsorption and/or desorption capacity should be considered when determining the amount of alginates in an application. Similar to Wang et al., (2018a), a 4:1 ratio was considered in the current adsorption-desorption and soil amendment studies to increase the adsorption capacity of BAC without increasing the cost substantially. Adding alginates with biochar did increase the maximum adsorption by 70.0 % compared to biochar alone which was similar to the previous studies where a 88.0 and 82.0 % increases were found using BAC compared to biochar alone (Do & Lee, 2013; Wang et al., 2018a). For the adsorption and desorption experiments, biochar was difficult to separate from Pb^{2+} and HNO_3 solutions, respectively, resulting in biochar particles stuck inside the 50 mL tubes. Moreover, the transition of biochar from the weighing tins also resulted in some biochar lost. The addition of alginates functioned as a stable matrix for biochar (Wang et al., 2019b) and eliminated the loss of biochar when separating from the aqueous solution and regenerating. Alginates also reduced the time spent separating biochar form the aqueous solution. Biochar required 2 h of centrifuging and another 2 h of filtering whereas BAC needed less than 10 min to be filtered twice. Overall, the addition of alginates made biochar easier to handle, reduced the adsorption and desorption experimental time, increased adsorption and desorption capacity, and reduced the loss of biochar. Moreover,

the lower cost of biochar renders the BAC to be cost-effective (Do & Lee, 2013; Wang et al., 2018a) and therefore, worth using alginates.

4.5. Conclusion

The current chapter focused on the how the characterization and form of biochar and alginates impacted the sorption dynamics and also compared the use of alginates with biochar. Biochar exhibited wood capillaries with an irregular nonuniform size where the addition of alginates encapsulates the biochar and provides a smooth barrier over the wood capillaries. Biochar and BAC had the capability to adsorb almost 95.0 % of each Pb^{2+} concentration and Pb^{2+} spiked biochar and BAC had the capability to release up to 68.4 and 79.6 % of Pb^{2+}, respectively, in a short period of time. Except for the desorption of BAC, Langmuir isotherm was a better fit and found BAC to have a higher maximum adsorption and desorption capacity. The concentration of Pb^{2+} demonstrated a positive correlation with biochar & BAC adsorbing Pb^{2+} and BAC demonstrated superior adsorption capacity of Pb^{2+} than biochar alone therefore, both hypotheses for the first study were accepted. Furthermore, alginates were determined to be of value and enhance the form and sorption dynamics of biochar. The next chapter will consider the release and transport of Pb^{2+} from spiked biochar and BAC after application to soil.

5. Release and Transport of Pb^{2+} in Spiked Biochar and BAC Amended Soils and Effects on Soil Microbial Respiration

5.1. Introduction

Over the past decades, poor agricultural management has led to the accelerating degradation in soil quality (Bauer et al., 2006). Many studies have aimed to improve organic carbon in soil by adding amendments originating from waste biomass sources (Zhang et al., 2019). Biochar, a result of pyrolyzing biomass feedstocks, has attracted increasing attention for soil remediation due to the stable carbon (C) compounds, reactive surfaces, and surface structures (Zhang et al., 2019). As a promising soil amendment, biochar has been widely applied to: 1) Improve soil structure and fertility (Chan et al., 2007; Lehmann et al., 2006); 2) Promote C sequestration (Lehmann, 2007b); 3) Mitigate nutrient leaching and improve microbial activity (Lehmann, 2007a); and 4) Remediate soil contaminated with heavy metals (Srinivasan et al., 2015). Moreover, biochar has been applied in aqueoues solutions, including wastewater, for remediation of heavy metals. Some recent studies have included the addition of alginates with biochar to create composites that have a bead-like structure. Together, biochar and alginates form a biochar-alginate composite (BAC) that has been shown to be an efficient adsorbent for Pb^{2+} removal from aqueous solutions (Do & Lee, 2013). However, investigating the impacts Pb^{2+} contaminated biochar or BAC have on soils after they have been used in water remediation of heavy metals has not be researched**.** Two promising studies investigated the effect of agricultural soil amended with ash and biochar from artificially contaminated wood (Jones & Quilliam, 2014; Lucchini et al., 2014). The studies examined the metal bioavailability, crop growth, and soil microbial activity with various

heavy metals including As, Cd, Ni, and Pb. The bioavailability of heavy metals was significantly higher in contaminated wood ash soil treatments compared to contaminated biochar (Jones & Quilliam, 2014; Lucchini et al., 2014). Furthermore, the availability of As, Cd, Ni, and Pb appeared to be lower in soils treated with heavy metal contaminated biochar relative to untreated soil (Lucchini et al., 2014).

In the previous chapter, birch biochar and BAC were mixed with Pb^{2+} solutions ranging from 5 to 94 $\mu g\ L^{-1}$. Biochar and BAC adsorption capacities were found to be approximately 94.6 and 94.2 %, respectively, and the desorption capacities were found to be approximately 68.4 and 79.6 %, respectively. Both adsorbents possessed the capability to adsorb and desorb large quantities of Pb^{2+} however, the adsorption capacity of both adsorbents were much greater. The objective was to investigate the impacts Pb^{2+} spiked biochar and BAC have when applied to soil. The current study will assess the leaching and bioavailability of Pb^{2+}, and microbial respiration of soil after Pb^{2+} spiked biochar and BAC were released in soil. Considering the previous study, it was hypothesized treatments more likely to desorb Pb^{2+} will have a higher amount of Pb^{2+} leach from the soil and soils amended with Pb^{2+} spiked BAC will have greater microbial respiration. We also hypopthesized as Pb^{2+} concentration increases, Pb^{2+} will inhibit carbon release when soils are amended with Pb^{2+} spiked biochar & BAC.

5.2 Materials & Methods

5.2.1. Chemical Reagents

Calcium chloride ($CaCl_2$, 96% of purity) and sodium alginate were purchased from Acros Organics - Fisher Scientific Co. (Ottawa, ON, Canada) where the sodium alginate was extracted from brown algae in powder form and was not further purified.

Nitric acid (HNO_3, ≥98% of purity), sodium hydroxide (NaOH, ≥97% of purity), and Pb^{2+} (SPEXertificate, 1000 μg mL^{-1}) were also purchased from Fisher Scientific Co. (Ottawa, ON, Canada).

5.2.2. Biochar & Biochar-Alginate Bead Preparation

Please see section 4.2.2. and 4.2.3. for biochar and biochar-alginate composite (BAC) bead preparation, respectively.

5.2.3. Spiking Biochar & BAC with Pb^{2+}

Stock solutions of Pb^{2+} (1000 μg mL^{-1}) were prepared by dissolving Pb^{2+} with deionized water creating desired solutions of 10 and 100 μg L^{-1}. The leaching and microbial respiration experiments used Pb^{2+} spiked biochar and BAC at two concentrations (10 and 100 μg L^{-1}) and a control group (0 μg L^{-1}) where the adsorbents were placed in unspiked deionized water. The experimental units were placed randomly to create a Completely Randomized Design (CRD). Each experimental unit had a dry weight of 0.05 g and they were placed into 50 mL Pb^{2+} spiked solutions at 0, 10, and 100 μg L^{-1}. The pH of each experimental unit was adjusted to 5.0 ± 0.2 with the addition of HNO_3 and NaOH. Biochar and BAC experimental units in the spiked solutions were shaken in 50 mL tubes placed horizontally at 60 rpm at room temperature (20°C) using a benchtop Eberbach Corporation Shaker (115 volts, 07047 A5407WVS, Van Buren Charter Township, MI, United States). In the sorption-desorption experiments (Chapter 4), biochar and BAC reached adsorption equilibrium in 7 and 1 day(s), respectively. The same amount of time to spike the adsorbents in the adsorption experiment was applied in the present leaching and microbial respiration experiments. Thus, for the following leaching and microbial respiration experiments, biochar and BAC experimental units

were shaken: a) 7 days; and b) 1 day; in 50 mL spiked Pb^{2+} solution. After shaking, the 50 mL biochar experimental units were centrifuged using an International Centrifuge Tachometer from International Equipment Co. (Boston, MA, United States) for 2 h. BAC experimental units were filtered with Q2 Quantitative filter papers from Fisher Scientific Co. (Ottawa, ON, Canada) to separate adsorbents from the aqueous solution. After adsorption, the aqueous solutions were acidified with HNO_3 to 1 % (v/v) and stored in refrigerators at 2 °C until they were ready to be analyzed.

5.2.4. Leaching Column Experimental Design

In total, 126 destructive experimental units in triplicates were established for a 28-day incubation study and they were sampled at 4-day intervals. The treatments were randomly placed in the laboratory but the experimental units were arranged by their 4-day sampling intervals due to the high number of experimental units (Figure 19). PVC pipes with a 3.18 cm diameter were cut into 12.1 cm length pieces. A mesh screen and filter were attached to the bottom of each PVC pipe to prevent loss of soil. Spiked biochar and BAC, described in section 5.2.3., were mixed separately with 100 g of wet soil. Wet soil was used to mimic the natural state of soil outside. The soil was obtained from an agricultural field in Innerkip, Ontario with a grey-brown podzols texture. The soil had a gravimetric moisture content of 16.7 % which was indicated in Table 5. A treamtent, denoted as 0 $\mu g\ L^{-1}$, was the control group which represented the unspiked biochar and BAC in soil control groups (an unspiked and unamended soil control was not included). In total, there were six soil treatments: 1) BC-0; 2) BC-10; 3) BC-100; 4) BAC-0; 5) BAC-10; and 6) BAC-100. The experimental units were filled into the PVC pipes and the bottom of the PVC pipes were attached to a 1 L mason jar to capture any

solution passing through. Deionized water was poured daily into each PVC pipe to represent rainfall conditions. Parafilm from Fisher Scientific Co. (Ottawa, ON, Canada) covered the top of each PVC experimental unit to retain moisture and was removed for 1 h each day. Deionized water was added during the 1 h aeration period.

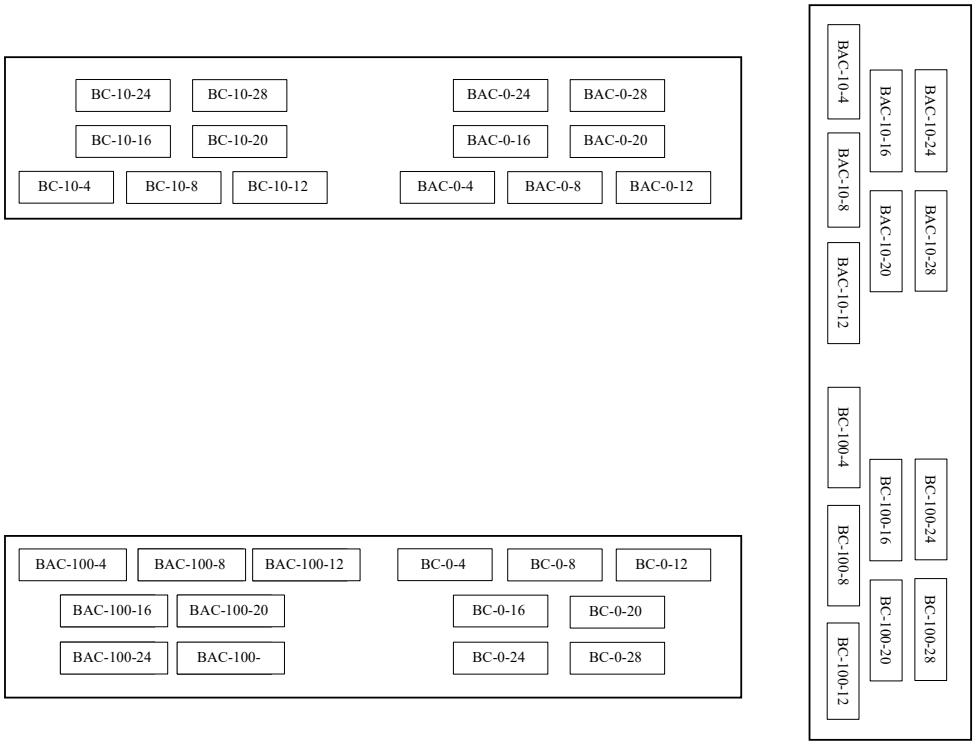

Figure 19. Leachate floorplan of experimental units where the treatment sections are randomly chosen and experimental units are organized by sampling intervals (n=3).

Figure 20. Leaching Experimental Setup. BAC-10 treatment section at day 3 with a total of 18 experimental units.

The amount of deionized water poured daily was based on the average rainfall per day on an annual basis in Oxford County, Ontario, where Innerkip is located. Rainfall amount was calculated by following equation:

$$\text{Rainfall Water Volume} = (\text{PVC Pipe Area}) \text{ x } (\text{Rainfall Depth}) \quad (6)$$

$$\text{Rainfall Water Volume} = (2\pi rh + 2\pi r^2) \text{ x } (\text{Rainfall Depth})$$

$$\text{Rainfall Water Volume} = ((2\pi(1.5875\text{cm})(12.065\text{cm})) + (2\pi(1.5875\text{cm})^2)) \text{ x } (2.5\text{cm})$$

$$\text{Rainfall Water Volume} = 30.75 \text{ mL}$$

The volume of water calculated was 30.75 mL per day and the full amount of deionized water was poured on the surface of the soil in the PVC pipe. A 10 mL volumetric pipette from Fisher Scientific Co. (Ottawa, ON, Canada) was used to slowly dispense the deionized water on the soil. After each 4-day sampling interval, 18 experimental units were removed from the incubation period and the leachate was collected from the mason

jar. The PVC pipe was detached from the mason jar and the leachate was poured into a volumetric cylinder to determine the volume. After recording the volume, the leachate was transferred into a 250 mL container and acidified with HNO_3 to 1 % (v/v). Experimental units were stored in a refrigerator at 2 °C until the end of the 28 days when all experimental units were analyzed.

Table 6. Innerkip, Ontario soil chemical and physical properties.

Soil Category	Grey-brown Podzol
pH	7.12
Na (kg ha^{-1})	27
Ca (kg ha^{-1})	6077
Mg (kg ha^{-1})	496
K_2O (kg ha^{-1})	193
P_2O_5 (kg ha^{-1})	593
Zn (ppm)	8.78
Fe (ppm)	235
Al (ppm)	665
B (ppm)	1.23
Cu (mg kg^{-1})	7.01
Mn (ppm)	108
CEC (m_{eq}/100g)	18.0
MC (%)	16.7
Organic Matter (%)	4.30
Density (g cm^{-3})	1.24

5.2.5. Microbial Respiration Experimental Design

The measurement of microbial activity is a valuable tool to assess the biological state and health of soil (Bauer et al., 1991) where an increase in CO_2 respiration indicates greater microbial activity that is attributed to consumption of carbon (C) from the organic C pool in soil (Haney et al., 2018). The C portion of the released CO_2 (mg) in this study was measured using SCD30 sensors (SCD30, CO_2 accuracy (± 30 ppm +3% MV) @ 400-10,000 ppm) from Sensirion (Chicago, IL, United States) to determine if Pb^{2+} spiked biochar and BAC stimulated or inhibited the microbial activity in the soil. In total, 21

experimental units were established, and similar to the leaching experiment, the microbial respiration experiment had a 28-day incubation period. However, the last week of the incubation showed large variability in the results due to environmental changes occurring in the space. On day 21 of the experiment, a spike was seen in the experimental data and continued for the following two days. On day 24, random spikes were seen again in the experimental unit data which no longer followed the aeration trend of the data. Furthermore, the microbial respiration was on a downward trend which could no longer be seen at day 21 of the experiment and random spikes occurred until the end of the 28-day experiment. The laboratory space was shared with other students who stored vehicles and kept garage doors opened for long periods of time. Their activities could have caused the sporadic increases seen in C released near the end of the experiment and therefore, only the results for the first 20 days of the experiment were considered. Spiked biochar and BAC, described in section 6.2.3., were mixed separately with 100 g of wet soil. The same soil from the leaching experiment was used and had the same gravimetric moisture content of 16.7 % which is indicated in Table 5. In total, there were 7 soil treatments: 1) BC-0; 2) BC-10; 3) BC-100; 4) BAC-0; 5) BAC-10; 6) BAC-100; and 7) soil. BC and BAC represent biochar and biochar-alginate composite materials, respectively, the 0 represents the control group of unspiked adsorbents with soil, 10 and 100 represent the two Pb^{2+} spike concentrations ($\mu g\ L^{-1}$) added to the soil, and the soil represent the control group without Pb^{2+} or adsorbents. Each soil treatment was placed into a 250 mL mason jar and a 250 mL clear plastic cup, with the bottom cut off, was placed on top of the jar.

Figure 21. Mixing Pb^{2+} spiked BAC with soil before putting into mason jars for microbial respiration experiment.

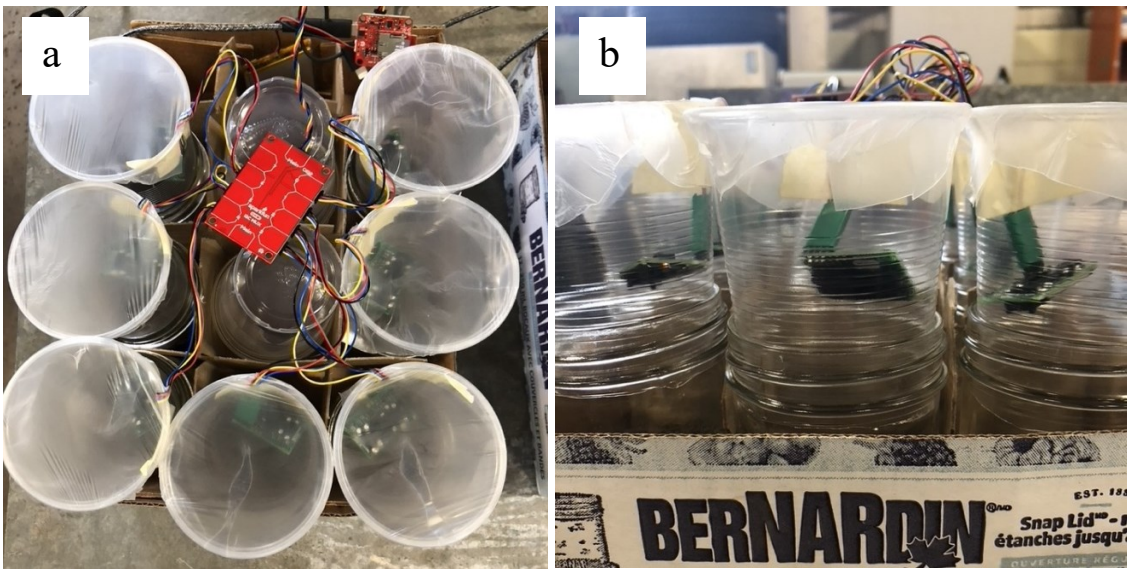

Figure 22. (a) Topview and (b) Sideview of microbial respiration experimental setup with sensors.

SCD30 sensors were taped to the inside of the plastic cup to measure CO_2, relative humidity, and temperature over the experimental period. The sensors were connected to an eight port multiplexer (Qwiic Mux Breakout - 8 Channel, TCA9548A) and a data logger (OpenLog Artemi) from SparkFun (Boulder, CO, United States). The loggers were recording data at 5 min intervals continuously over the whole experiment. Parafilm from Fisher Scientific Co. (Ottawa, ON, Canada) covered each plastic cup during the 28-day soil respiration experiment to retain moisture but was removed for 1 h each day to introduce fresh air into the vessels.

5.2.6. Data Analysis

Stock solutions and leachate experimental units were analyzed using an Agilent 7800 ICP-MS (1500 W RF power, 10 mm sample depth, 206, 207, 208 isotopes, internal Bi standard) in the Department of Chemistry at the University of Acadia (Wolfville, NS, Canada). Pb^{2+} was measured as the sum of isotopes 206, 207, and 208, and Bi-209 was used as an internal standard). QA/QC protocol incorporated a certified reference material (simulated natural water: CRM-TMDW-A, High-Purity Standards) which was traceable to the NIST 3100 series, reagent blanks, and continuing calibration verification to assess method accuracy. Recoveries were typically within ±10 % of the accepted value. In addition, a duplicate soil sample to monitor analytical precision and a method blank to measure background was analyzed once every ten samples. Stock solutions were analyzed prior to spiking biochar and BAC to ensure desired spike Pb^{2+} concentrations were obtained.

Microbial respiration data was extracted weekly from each logger. Microbial respiration was measured in the form of CO_2 using SCD30 sensors where CO_2 data was converted from ppm into mg of CO_2-C. The mass of CO_2 released was calculated by:

$$\mathrm{CO_2\ (mg)} = \frac{\text{Volume of Gas in Jar } (cm^3) \text{ x Experimental Unit } \mathrm{CO_2\ (mg\ L^{-1})}}{1000} \quad (7)$$

Followed by calculating the moles of CO_2:

$$\mathrm{CO_2\ (moles)} = \frac{\text{Pressure (atm) x } \frac{\mathrm{CO_2\ (mg)}}{1000000}}{\text{Temperature (K) x Gas Constant (L atm } \mathrm{K^{-1}mol^{-1}})} \quad (8)$$

Followed by calculating the mass of CO_2-C:

$$\mathrm{CO_2 - C\ (mg)} = \mathrm{CO_2\ (mol)} \text{ x Carbon Molar Mass (g } \mathrm{mol^{-1}}) \text{ x } 1000 \quad (9)$$

5.2.7. Statistical Analysis

All experimental units were replicated three times and the average experimental data was used for statistical analyses. Relative standard deviation between triplicates and confidence levels were determined using Minitab® Statistical Software Web App. Different factors of interest were used for repeated measures analysis of variance, ANOVA, which included adsorbent material type (biochar and BAC), Pb^{2+} concentrations (0, 10, and 100 μg L^{-1}), and time (4, 8, 12, 16, 20, 24, 28 days). A CRD model was used and the model's compliance was determined using the Anderson-Darling Normality test. If the assumption of normality and constant variance were verified ($\rho \geq 0.1$) a comparison by Fisher's Least Significant Difference test was completed to calculate the differences between means at a significance level of $\alpha = 0.05$. However, if the assumption of normality and constant variance were violated ($\rho \leq 0.1$), data transformations were conducted on the response variables. Furthermore, if the treatments

significantly impacted the sorption capacity ($\rho \leq 0.05$), means of the triplicate experimental units were compared with the Least Square Means test.

5.3 Results

5.3.1. Pb^{2+} Content

Results in the previous chapter found birch biochar contains small concentrations of Pb^{2+} prior to spiking the material. The mean concentration measured in the desorption experiment from biochar and BAC was 3.19 ± 0.200 and 1.51 ± 0.0400 μg L^{-1}, respectively. The results from the leaching experiment in Figure 23 and 24 further supports Pb^{2+} presence in biochar and potentially soil since the control group, 0 μg L^{-1}, which had unspiked biochar applied to soil, had traces of Pb^{2+} in the leachate. A total of 1.77 and 1.88 μg were found in the BC-0 and BAC-0 μg L^{-1} treatments, respectively, where only 0.174 and 0.0730 μg of Pb^{2+} were added by biochar and BAC, respectively. Although a soil control group was not included in the leaching experiment, there was a minimum of 1.60 and 1.80 μg of Pb^{2+} in the soil prior to being applied by spiked adsorbents. The same trend was seen in each treatment where the total amount of Pb^{2+} leaching from soil increased with time however, there was a decrease in the treatments every 12 days. Except for BC-10 treatment, BAC leached slightly higher amounts of Pb^{2+} throughout the experiment. BC-0 and BAC-0 treatments had higher amounts of Pb^{2+} leached from the soil for the majority of sampling periods. No significant 3-way interaction effect occurred ($p=0.354$) however, 2-way interaction effect happened between sampling periods and Pb^{2+} concentration ($p=0.007$), and adsorbent and Pb^{2+} concentrations ($p=0.027$). BAC-100 and BAC-10 had the highest and least amount of Pb^{2+} leach from the soil, respectively, compared to all other treatments. Furthermore, the

first 12 days of the experiment, most of the treatments are significantly lower from the remaining 16 days.

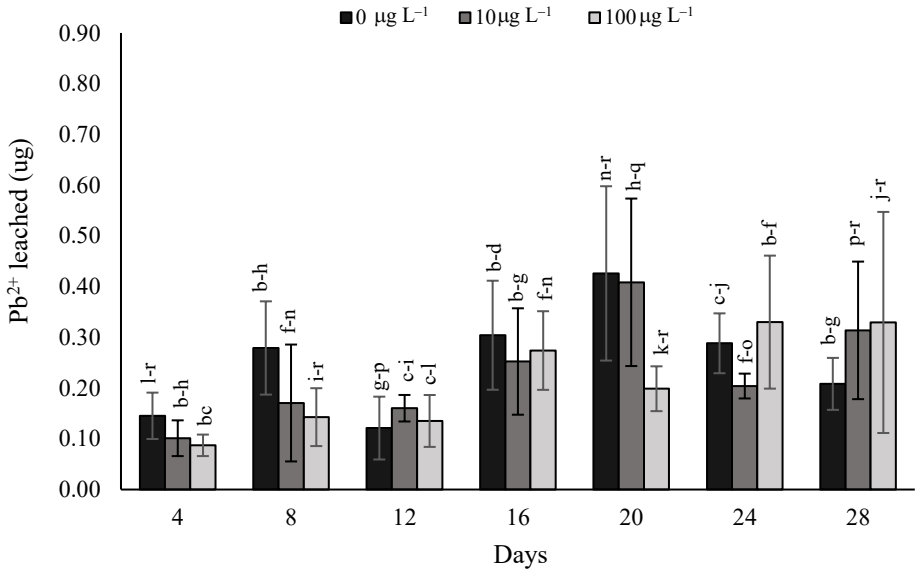

Figure 23. Total amount (µg) of Pb^{2+} leaching per 4-day intervals from soil with Pb^{2+} spiked biochar throughout the 28-day experiment from a 3-way interaction of adsorbent x sampling period x Pb^{2+} concentration. Different letters indicate significant differences ($p<0.05$) across concentrations and time. Vertical bars represent the standard deviation (n=3).

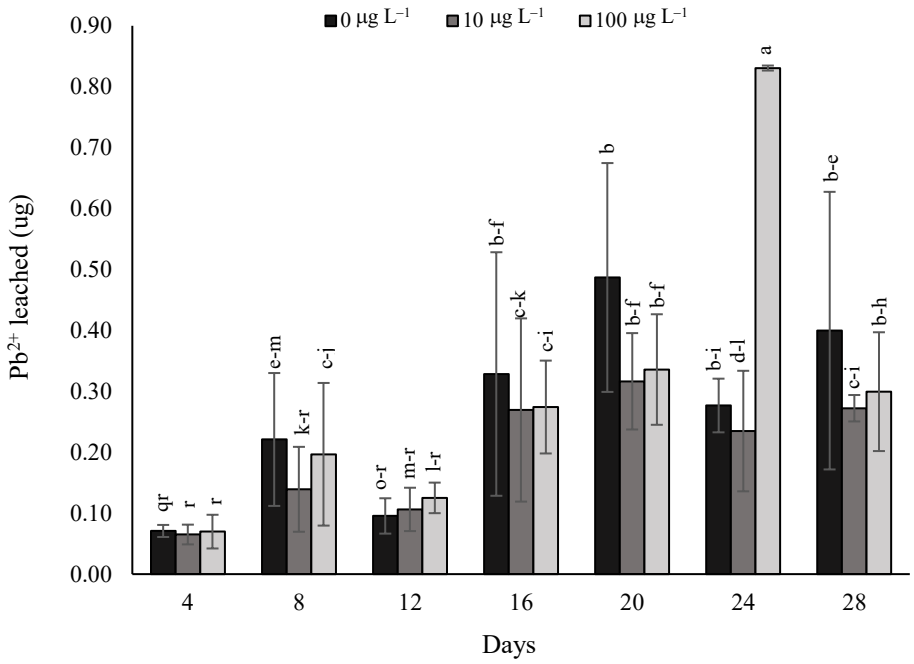

Figure 24. Total amount (µg) of Pb^{2+} leaching per 4-day intervals from soil with Pb^{2+} spiked BAC throughout the 28-day experiment from a 3-way interaction of adsorbent x sampling period x Pb^{2+} concentration. Different letters indicate significant differences ($p<0.05$) across concentrations and time. Vertical bars represent the standard deviation (n=3).

5.3.2. Pb^{2+} Bioavailability

Bioavailability of Pb^{2+} was the portion of Pb^{2+} able to be desorbed from the adsorbents and released into soil solution as a soluble metal. Unlike the previous other studies, soil did not demonstrate a significant pH spike when biochar and BAC were initially added. In the current experiment, Pb^{2+} spiked biochar and BAC had a lower initial pH range of 6.8 to 7.2 compared to Lucchini et al., (2014) and Jones & Quilliam (2014) findings. Biochar and BAC mixed into the soil matrix did not increase the pH by the end of the experiment which was similar to Lucchini et al., (2014) and Jones & Quilliam (2014) findings. The bioavailability at the end of the experiment was similar between all the treatments regardless of the amount of Pb^{2+} spiked in biochar (Figure 25) and BAC (Figure 26), with a range of 0.0170 to 0.0220 µg g^{-1}. Therefore, increasing the

Pb^{2+} concentrations by one and two magnitudes into the soil spiked with biochar and BAC did not impact the Pb^{2+} bioavailability. Throughout the 28-day experiment, Pb^{2+} bioavailability remained within 70 and 140 μg g^{-1} for the acceptable limits for total amount of Pb in agricultural and residential soil, respectively, as set by the CCME (CCME, 1999).

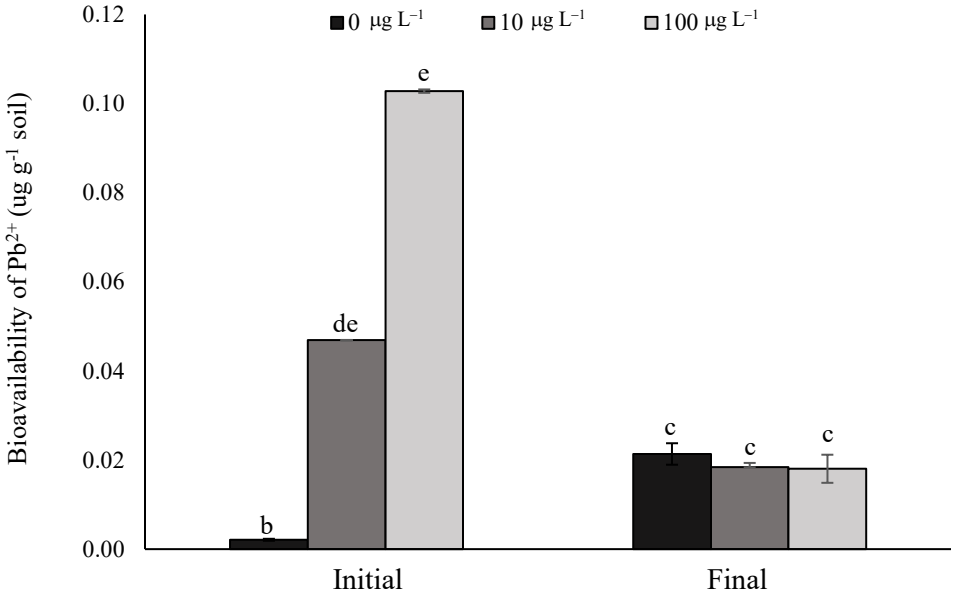

Figure 25. Total Pb^{2+} bioavailability in soil with Pb^{2+} spiked biochar at 0, 10, and 100 μg L^{-1} concentrations at the beginning and end of the leching experiment. Different letters indicate significant differences ($p<0.05$) across concentrations and time. Vertical bars represent the standard deviation (n=3).

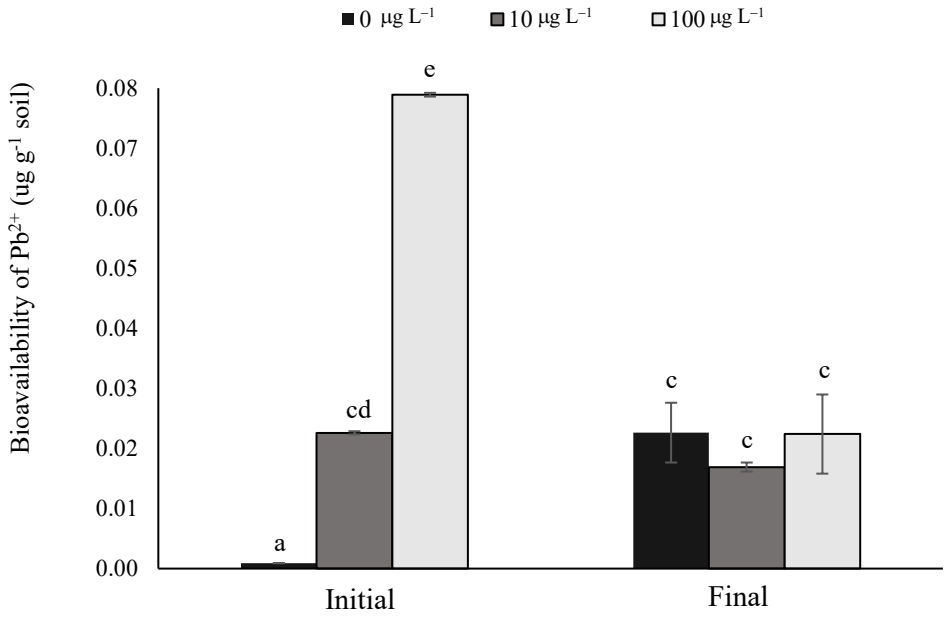

Figure 26. Total Pb^{2+} bioavailability in soil with Pb^{2+} spiked BAC at 0, 10, and 100 μg L^{-1} concentrations at the beginning and end of the leching experiment. Different letters indicate significant differences ($p<0.05$) across concentrations and time. Vertical bars represent the standard deviation (n=3).

5.3.3. Microbial Respiration in Soil

Both the adsorbents and rates of spiked Pb^{2+} had significant effects on soil microbial respiration throughout the 28-day experiment relative to the control soil group (Figure 27). Carbon mineralization (CO_2-C) at 10 and 100 μg L^{-1} of Pb^{2+} spiked BAC had closer CO_2-C emissions than either Pb^{2+} spiked biochar treatments. Therefore, BAC stimulated higher microbial respiration than any spiked or unspiked Pb^{2+} biochar treatment. CO_2-C emissions were higher for Pb^{2+} spiked biochar and BAC at 10 μg L^{-1} than at 100 μg L^{-1} concentration. A decrease in microbial respiration of approximately 4 % was found as the Pb^{2+} concentration increased from 10 to 100 μg L^{-1} for both adsorbents. The soil control group had the lowest amount of C detected with only approximately 245 mg of CO_2-C released and unspiked biochar and BAC had microbial respiration, i.e. CO_2-C release, more than 3 times greater than from soil alone.

Furthermore, Pb^{2+} spiked biochar and BAC at 10 μg L^{-1} had CO_2-C production 5 and 6 times greater than the soil control group, respectively.

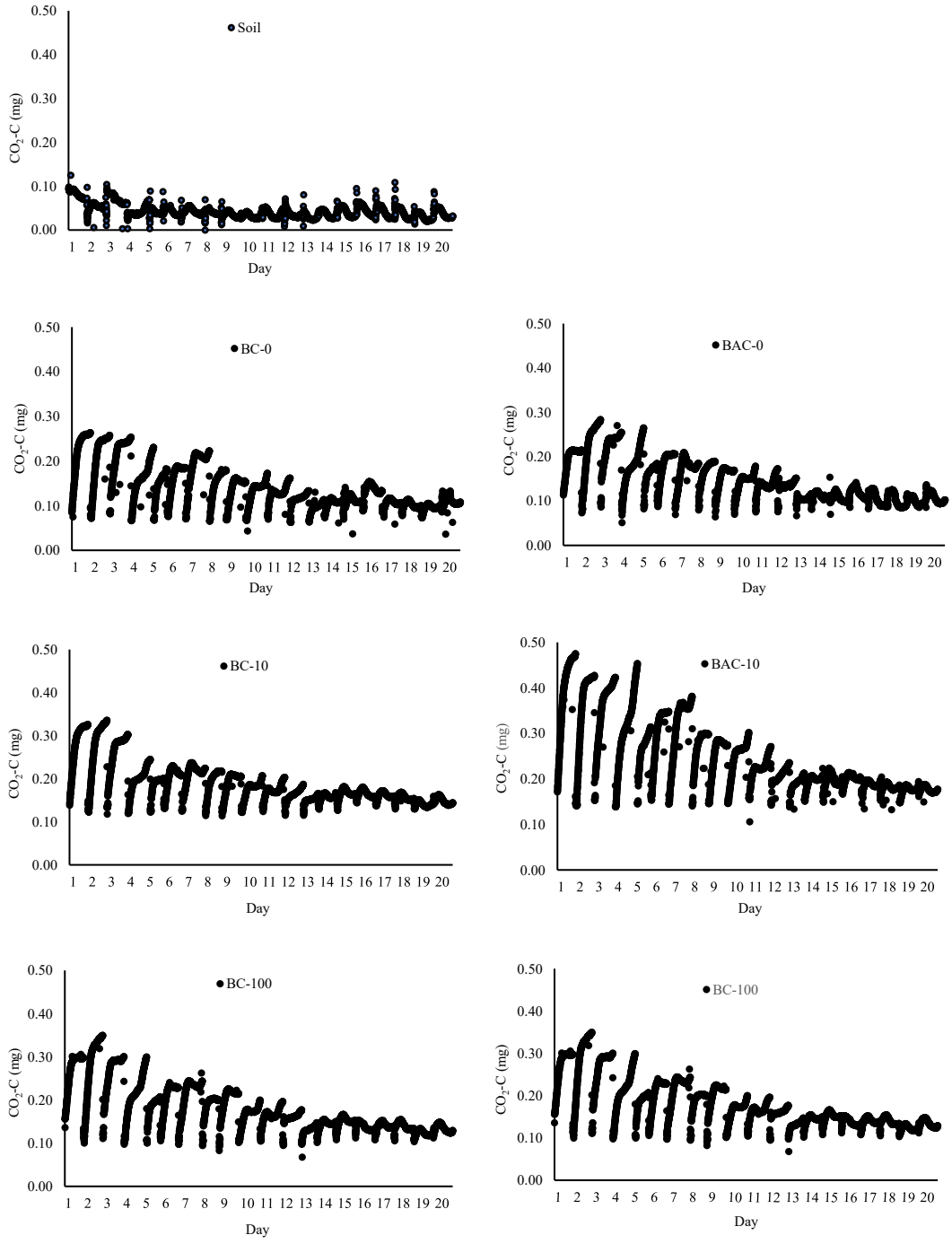

Figure 27. Total CO_2-C (mg) released from each treatment, Soil, BC-0, BAC-0, BC-10, BAC-10, BC-100, and BAC-100 applied to soil over the 20-day incubation period microbial respiration experiment. Each day represents a 24-h measurement period (n=3).

5.4. Discussion

5.4.1. Effect of pH on Pb^{2+} Bioavailability

Biochar has been studied as both a soil and water amendment. Applying biochar to soil improves microbial respiration, increases organic C, and CEC (Sohi et al., 2010); and applying biochar with alginates to contaminated water enhances the rate of metal uptake and generates a higher density particle (Biswas et al., 2019). The aim of this study was to remove Pb^{2+} from water using biochar and alginates, and determine the potential for release of the Pb^{2+} contaminated adsorbents into soil. Generally, leached concentrations of the heavy metals were significantly lower than the total initial concentrations and demonstrate a strong pH-dependence (Dijkstra et al., 2004). The Pb^{2+} bioavailability in the biochar (Figure 25) and BAC (Figure 26) was extremely low which was a result of the soil and biochar pH levels. The pH of soil can influence the mobility and availability of Pb^{2+} in soil (CCME, 1999). Concentrations of heavy metals have the potential to drop more than 2 orders of magnitude between pH 2.0 to 7.0 and increase again as the pH level becomes more alkaline (Dijkstra et al., 2004). With an increase in pH, the retention of heavy metals on soil particles increases and the pH-dependent negative charge on soil surface also rises; therefore, stimulating further sorption and the immobilization of metals from biochar in the soil (Lucchini et al., 2014; Rees et al., 2014). Two studies found using Cu spiked biochar derivied from Cu-treated wood had minimal lasting effects on heavy metal bioavailability for As, Cd, Ni, Pb, and Zn in a sandy clay loam soil however, a significant increase in Cu was seen in soil amended with Cu-treated wood biochar from the beginning to the end of the experiment (Jones & Quilliam, 2014; Lucchini et al., 2014). Opposite results were found in the current

leaching experiment as Pb^{2+} availability decreased throughout the experiment and continued to be low at the end. Biochar and soil had a pH level of 5.0 ± 0.2 and 7.1, respectively, where the final leachate values ranged between 6.8 to 7.2 which supports the expectation that heavy metal solubility decreases with a rise in pH of biochar and/or soil. In the current study, Pb^{2+} was unknowingly present in the biochar product and upon further investigation it was determined that the biochar and BAC had an average concentration of 3.19 ± 0.200 and 1.51 ± 0.0400 μg L^{-1}, respectively. The maximum amounts of Pb^{2+} leached were 1.85 and 1.15 μg L^{-1} for biochar and BAC, respectively. Therefore, both the initial biochar Pb^{2+} concentration and the spiked Pb^{2+} proportion in biochar and BAC did not desorb and leach from the soil early in the study. Over the 28-day experiment, Pb^{2+} did desorb and re-adsorb at certain incubation intervals as demonstrated in Figures 23 and 24. Minimal bioavailable Pb^{2+} leached from the soil was evident by the end of the incubation period and again, supports the observations that heavy metal solubility decreases or halts with a pH rise in biochar and/or soil.

5.4.2. Microbial Respiration from Pb^{2+} Spiked Biochar and BAC

In this microbial respiration experiment, CO_2 gas released was measured using SCD30 sensors and the C portion was calculated to determine whether the addition of Pb^{2+} spiked biochar and BAC impacted the microbial community. The hypothesis that soils amended with Pb^{2+} spiked BAC will have greater microbial respiration was accepted since there was more than 3 times carbon mineralized (CO_2-C) with the addition of biochar and/or BAC relative to soil control group. However, in the short-term, greater soil respiration was not necessarily desirable. Greater soil respiration can suggest unstable soil structure or environment, such as when microbial cells die and undergo

rapid turnover as they decompose (Service United States Department of Agriculture Natural Resources Conservation, 2014). The measured soil respiration could signify a strong stimulation of soil microorganisms by biochar and BAC (Steinbeiss et al., 2009). The increase in respiration could be a function of stimulation from the adsorbents and/or Pb^{2+} removing and consuming certain microbial groups. In the current experiment, there was a 69.5 and 70.9 % increase in microbial respiration when biochar and BAC were included in the soil, respectively. Adding 10 μg L^{-1} of Pb^{2+} increased microbial respiration by 7.69 and 11.7 % with biochar and BAC, respectively, further increasing the total microbial respiration to 77.3 and 82.9 %, respectively. Furthermore, increasing Pb^{2+} concentration from 10 to 100 μg L^{-1} decreased the microbial respiration by 4.20 and 4.05 % with biochar and BAC, respectively. Biochar, alginates, and Pb^{2+} stimulated microbial respiration of soil where the alginates further increased the CO_2-C released by 5.73 and 1.35 % with and without Pb^{2+} present, respectively. Alginates, specifically sodium-alginate which was used in the current experiment, have an abundant of free hydroxyl and carboxyl groups (Wang et al., 2019b). Carboxyl groups have the ability to experience a chemical reaction and release CO_2. BAC had more C sources compared to biochar and the addition of sodium-alginates could be the cause of the increased release of CO_2-C in the BAC treatments. The stimulation from the adsorbents had a greater impact on microbial respiration than Pb^{2+} where the addition of Pb^{2+} caused microbial respiration to decrease once Pb^{2+} passed a certain threshold between 10 and 100 μg L^{-1}. Increasing the concentration could have caused more space to be occupied by Pb^{2+} which provided less space for other organisms to occupy and could be the result of the decrease in microbial respiration seen. The increase in microbial respiration causes greater amounts of CO_2 to

be released from the soil which increases the total C loss. The loss of carbon can impact soil structure, nutrient cycling, soil's fertility, and biodiversity for microorganisms which diminishes the quality of the soil. Biochar provides enough C that the increase of C lost still provides more C in the soil than soils without biochar. The increase in C losses due to the addition of biochar was also seen in Steinbeiss et al., (2009) where the study focused on the microbial activity and carbon balance of soils amended with two different types of biochar. The study found even with an increase in C turnover, the total C in soil was 27.0 % and 23.0 % higher with glucose-biochar and yeast-biochar treatments, respectively, compared to the controls at the end of the experiment.

Service United States Department of Agriculture Natural Resources Conservation (2014) determines a medium, ideal, and high level of microbial respiration to be between 500 to 1000, 1000 to 2000, and > 2000 mg CO_2-C per kg of soil per week, respectively. A medium, ideal, and high level of microbial respiration are defined as: soils that have moderately balanced conditions with organic matter; soils with adequate organic matter and active soil microorganisms; and soils with excessive organic matter, respectively (Service United States Department of Agriculture Natural Resources Conservation, 2014). In the current experiment, a rapid increase in microbial respiration was seen from the soil control group to soil mixed with biochar or BAC (Figure 28) which is partly due to the experimental setup. Biochar and BAC treatments released 4 to almost 8 times more CO_2-C and resulted in a total C loss 3 to 6 times higher than the soil alone. Therefore, within the incubation period of this experiment, biochar and BAC demonstrated high levels of microbial respiration which indicated a soil with more reactive organic matter and/or a potentially more unstable system, at the beginning. CO_2-C decreased sharply

each week for all treatments except the soil control group where CO_2-C production increased in the third week (Figure 28). A loss of C at a decreasing rate when applied with biochar has been observed in other studies (Jones & Quilliam, 2014; Steinbeiss et al., 2009; Wardle et al., 2008). One study found microbial respiration drastically decreased each week for the following 4 weeks and continually decreased for 12 weeks until a constant value was reached (Steinbeiss et al., 2009). Similarly in the current experiment, after three weeks, CO_2-C released decreased by almost half and plateaued. The changes seen in microbial respiration were quick due to the short experimental period. Although not conclusive, the experiments provided optimism moving forward with long-term experiments. Future experiments with several years are necessary to identify if carbon storage in soil improves with the addition of Pb^{2+} spiked biochar and BAC and if carbon storage will continue to gain significance over several years. The experiments need to identify if the C storage gain in the soil is more significant than the release of C. Furthermore, the experiments need to analyze the implication of Pb^{2+} in soil over 5 to 10 years and how much more Pb^{2+} could leach.

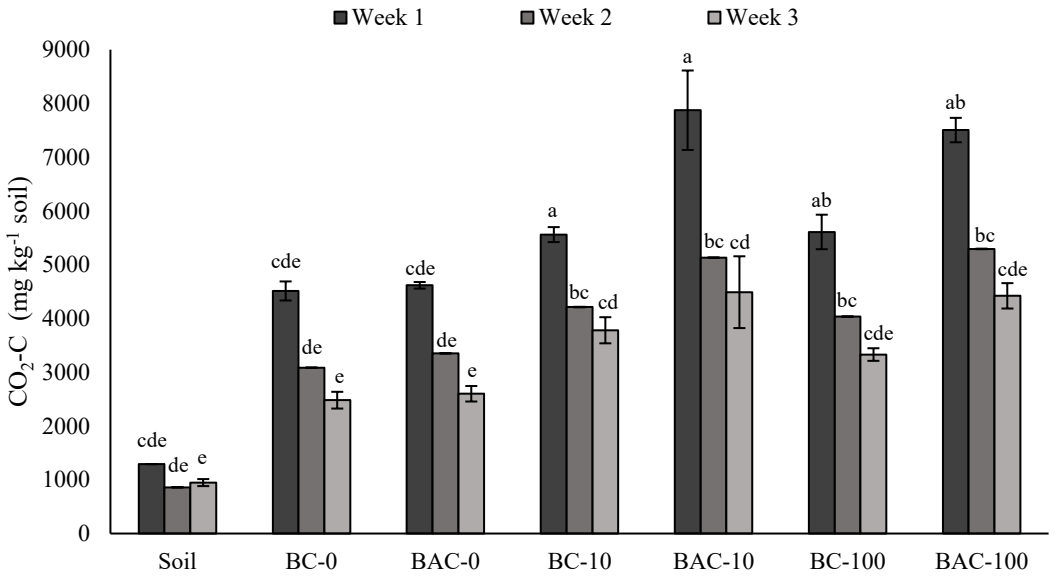

Figure 28. Total CO_2-C (mg) per kg of soil for each treatment, Soil, BC-0, BAC-0, BC-10, BAC-10, BC-100, and BAC-100, on a weekly basis during the incubation period of the microbial respiration experiment. Different letters indicate significant differences ($p<0.05$) across concentrations and time.

5.4.3. The Application of Pb^{2+} Spiked Biochar and BAC in Soil

Based on the results, Pb^{2+} spiked biochar and BAC applied to soil appeared to pose a low, short-term environmental risk, up to Pb^{2+} concentrations of 100 μg L^{-1} in relatively pH neutral soils. Therefore, on a short-term basis, releasing Pb^{2+} spiked biochar and BAC into soil was viable to recycle C back into the environment. Within 3 to 4 weeks, the maximum amount of Pb^{2+} leached from the soil from spiked Pb^{2+} biochar was extremely low and remained well below the acceptable Pb^{2+} limits in agricultural and residential soils (CCME, 1999). Furthermore, a boost in the release of CO_2-C, suggesting rapid initial microbial respiration, was not sustained and returned to pre-treatment levels. In the current experiment, the main challenge of Pb^{2+} spiked biochar and BAC in soil was the overall pH level. The type of soil, i.e. texture and chemical composition, and type of biochar determined the overall pH level which impacted the adsorption and desorption

abilities of biochar and BAC. Soils that have high alkalinity or acidity can increase desorbed Pb^{2+} and other heavy metals from biochar and BAC and increase their solubility. The pH of biochar and BAC can impact the amount of Pb^{2+} and other heavy metals adsorbed and retained by biochar and BAC. The change in the surface charge of biochar and alginates causes a decrease in sorption at lower and higher pH levels (Do & Lee, 2013; Issabayeva et al., 2006; Liu & Zhang, 2009; Wang et al., 2018a). In another study, Yang et al., (2021) studied biochar, with a pH of 9.9, applied to three different pre-contaminated Pb soils with pH levels of 5.8, 5.9, and 7.3. The soil that had a pH of 5.8 had 4.75 and 8.60 μg g^{-1} of Pb leach in the soil with and without the addition of biochar, respectively; the soil with a pH of 5.9 had 32.0 and 35.0 μg g^{-1} of Pb leach in the soil with and without the addition of biochar, respectively; and the soil with a pH of 7.3 had 80.0 and 150 μg g^{-1} of Pb leach in the soil with and without the addition of biochar, respectively. A decrease of Pb in the leachate was seen with the addition of biochar in the soil indicating biochar reduced the mobility of Pb however, the high alkalinity of biochar and the different soil types impacted the bioavailability of Pb differently (Yang et al., 2021). The pH of each soil changed from 5.8, 5.9, and 7.3 to 8.3, 8.8, and 8.4, respectively. In this case, biochar increased the pH of each soil matrix and stimulated greater precipitation of metal ions into soluble forms for the soil that had the highest pH initially (pH=7.3). In the current experiment, the pH of biochar (pH=5.0 ± 0.2) was more acidic than the soil (pH=7.1) and did not increase the pH of soil matrix. Therefore, a low stimulation of Pb^{2+} occurred when Pb^{2+} spiked biochar and BAC were released into the soil.

5.5. Conclusion

Biochar and biochar-alginate composite (BAC) were spiked with lead (Pb^{2+}) to investigate the impacts when released in soil by analyzing the release and transport of both spiked adsorbents. The microbial respiration experiment found BAC had more C sources compared to biochar due to the addition of sodium-alginates and BAC stimulated higher microbial respiration than any spiked or unspiked Pb^{2+} biochar treatment. Future investigations should include an alginate control group to identify how much alginates stimulate microbial respiration. The stimulation from biochar and BAC had a greater impact on microbial respiration than Pb^{2+} and the addition of Pb^{2+} caused microbial respiration to decrease once Pb^{2+} passed a threshold between 10 and 100 μg L^{-1}. The stimulation from biochar, BAC, and Pb^{2+} was likely not the same. A future study needs to identify the causes of stimulation and if the stimulation from the adsorbents and Pb^{2+} are different. Furthermore, the study needs to determine the amount of C released versus the amount of C added to soil when Pb^{2+} spiked biochar and BAC are released in soil over 5 to 10 years.

The leaching experiment further supported that Pb^{2+} was present in biochar and BAC, and traces of Pb^{2+} were also found in the soil prior to being applied by spiked adsorbents. With the exception of BC-10, BAC leached slightly higher amounts of Pb^{2+} throughout the experiment. Furthermore, increasing Pb^{2+} concentrations in the soil spiked with biochar and BAC did not impact Pb^{2+} leaching from the soil. With unknowingly having higher amounts of Pb^{2+} in the experiments, both the initial biochar Pb^{2+} concentration and the spiked Pb^{2+} proportion in both adsorbents did not desorb and leach from the soil early in the study. Over the 28-day experiment, Pb^{2+} did desorb and re-

adsorb at certain incubation intervals. The Pb^{2+} bioavailability in the biochar and BAC was extremely low which was a result of the soil and biochar pH levels. The bioavailability at the end of the experiment was similar between all the treatments regardless of the amount of Pb^{2+} spiked in biochar and BAC which remained within the acceptable limits set by the CCME. The pH of Pb^{2+} spiked adsorbents increased when mixed with soil and supported the expectation that heavy metal solubility decreases with a rise in pH of biochar and/or soil. The change of pH when spiked biochar and BAC was mixed with soil was the main physicochemical property changing the solubility and mobility of Pb^{2+}. Therefore, the type of soil and biochar, and their pH levels, determine the adsorbing and retaining amount of Pb^{2+} when releasing Pb^{2+} spiked biochar and BAC in soil. The main challenge in the future will be identifying exactly how long the changes in pH impact Pb^{2+} retained on biochar and BAC, and Pb^{2+} bioavailability in soil when spiked biochar and BAC are released in soil. Further investigations are needed to identify how much incremental changes in pH impacts solubility and mobility of Pb^{2+}. Specifically how much the pH of biochar impacts bioavailability of Pb^{2+} compared to the impact of soil's pH. Furthermore, the investigations need to expand their lifespan and study Pb^{2+} content and bioavailability from spiked biochar and BAC over a 5 to 10 year basis.

6. Conclusion & Recommendations

The current research was completed in two studies: 1) a adsorption-desorption kinetic study and 2) a biochar, BAC and soil amendment study. Study one focused on the how the characterization and form of biochar and alginates impacted sorption dynamics and assessed the use of alginates. Biochar and BAC had the ability to adsorb almost 95 % of each Pb^{2+} treatment and Pb^{2+} spiked biochar and BAC had the capability to release up to 68.0 and 79.0 % of Pb^{2+}, respectively, in a short period of time. Except for the desorption of BAC, Langmuir isotherm was a better fit and found BAC to have a higher maximum adsorption and desorption capacity. Alginates were found to be of value and enhance the form and sorption dynamics of biochar. Study two evaluated desorption and transport of Pb^{2+} from spiked biochar and BAC in soil columns and identified the effect of Pb^{2+} spiked biochar & BAC had on soil microbial activity. The microbial respiration experiment found BAC had more labile C sources compared to biochar due to the addition of sodium-alginates and BAC stimulated higher microbial respiration than any spiked or unspiked Pb^{2+} biochar treatment. The change of pH when spiked biochar and BAC were mixed with soil was the main physicochemical property changing the solubility and mobility of Pb^{2+}. Therefore, the main outcomes from the studies are: 1) Alginates added value and only BAC should be consider as an adsorbent moving forward; 2) Biochar, alginates, and Pb^{2+} stimulated microbial activity in the soil when applied; and 3) The type of soil and biochar, and their pH levels, determined the adsorbing and retaining amount of Pb^{2+} when spiked biochar and BAC are released in soil. The results identified in the adsorption-desorption and soil amendment studies provided optimism to continue moving forward. In the current research, a more alkaline

and/or neutral soil was considered to increase the pH of the Pb^{2+} spiked biochar and BAC solution which had an initial pH of 5.0. Due to time constraints, a local acidic soil was not included. Moving forward, a soil from Nova Scotia would be used. The pH of the Pb^{2+} spiked biochar and/or BAC solution would need to be manipulated to minimize solubility and mobility of Pb^{2+} in the acidic soil. The main challenge would be identifying the pH levels needed which includes the initial pH of biochar, pH of BAC, and pH of both Pb^{2+} spiked adsorbents. Furthermore, the results from the current research also lead to other questions: 1) With the addition of Pb^{2+} spiked BAC in soil, how much C is added to the soil versus the amount of C released from the soil?; 2) What causes the stimulation from biochar, alginates, and Pb^{2+} in microbial respiration and how do they differentiate?; and 3) How do all of these impact soil on a 5 to 10 year basis?. Applying these questions to the next studies will help further understand the implications of Pb^{2+} in soil when spiked BAC is applied to soil.

References

Ahmad, M., Lee, S. S., Dou, X., Mohan, D., Sung, J. K., Yang, J. E., & Ok, Y. S. (2012). Effects of pyrolysis temperature on soybean stover- and peanut shell-derived biochar properties and TCE adsorption in water. *Bioresource Technology*, *118*, 536–544. https://doi.org/10.1016/j.biortech.2012.05.042

Ahmad, M., Rajapaksha, A. U., Lim, J. E., Zhang, M., Bolan, N., Mohan, D., Vithanage, M., Lee, S. S., & Ok, Y. S. (2014). Biochar as a sorbent for contaminant management in soil and water: A review. *Chemosphere*, *99*, 19–33. https://doi.org/10.1016/j.chemosphere.2013.10.071

Ali, I. (2012). New generation adsorbents for water treatment. *Chemical Reviews*, *112*(10), 5073–5091. https://doi.org/10.1021/cr300133d

Ayawei, N., Ebelegi, A. N., & Wankasi, D. (2017). Modelling and Interpretation of Adsorption Isotherms. *Journal of Chemistry*, *2017*. https://doi.org/10.1155/2017/3039817

Babel, S., & Kurniawan, T. A. (2004). Cr(VI) removal from synthetic wastewater using coconut shell charcoal and commercial activated carbon modified with oxidizing agents and/or chitosan. *Chemosphere*, *54*(7), 951–967. https://doi.org/10.1016/j.chemosphere.2003.10.001

Banik, C., Lawrinenko, M., Bakshi, S., & Laird, D. A. (2018). Impact of Pyrolysis Temperature and Feedstock on Surface Charge and Functional Group Chemistry of Biochars. *Journal of Environmental Quality*, *47*(3), 452–461. https://doi.org/10.2134/jeq2017.11.0432

Barakat, M. A. (2011). New trends in removing heavy metals from industrial wastewater. *Arabian Journal of Chemistry*, *4*(4), 361–377. https://doi.org/10.1016/j.arabjc.2010.07.019

Bauer, E., Pennerstorfer, C., Holubar, P., Plas, C., & Braun, R. (1991). Microbial activity measurement in soil - a comparison of methods. *Journal of Microbiological Methods*, *14*(2), 109–117. https://doi.org/10.1016/0167-7012(91)90040-W

Bauer, P. J., Frederick, J. R., Novak, J. M., & Hunt, P. G. (2006). Soil CO2 flux from a norfolk loamy sand after 25 years of conventional and conservation tillage. *Soil and Tillage Research*, *90*(1–2), 205–211. https://doi.org/10.1016/j.still.2005.09.003

Biswas, S., Sen, T. K., Yeneneh, A. M., & Meikap, B. C. (2019). Synthesis and characterization of a novel Ca-alginate-biochar composite as efficient zinc (Zn 2+) adsorbent: Thermodynamics, process design, mass transfer and isotherm modeling. *Separation Science and Technology (Philadelphia)*, *54*(7), 1106–1124. https://doi.org/10.1080/01496395.2018.1527353

Canadian Council of Minister of the Environment. (1999). Canadian Soil Quality Guidelines for the Protection of Environmnetal and Human Health. *Canadian Environmnetal Quality Guidelines*, 10. http://energy.alberta.ca/BioEnergy/pdfs/HeavyMetalReport.pdf%5Cnhttp://ceqg-rcqe.ccme.ca/download/en/269

Carrier, A., Abdullahi, I., Hawboldt, K., Fiolek, B., & MacQuarrie, S. (2017). Probing Surface Functionality on Amorphous Carbons Using X-ray Photoelectron Spectroscopy of Bound Metal Ions. *Journal of Physical Chemistry C*, *121*(47), 26300–26307. https://doi.org/10.1021/acs.jpcc.7b06311

Carrier, M., Hardie, A. G., Uras, Ü., Görgens, J., & Knoetze, J. (2012). Production of char from vacuum pyrolysis of South-African sugar cane bagasse and its characterization as activated carbon and biochar. *Journal of Analytical and Applied Pyrolysis*, *96*, 24–32. https://doi.org/10.1016/j.jaap.2012.02.016

Chan, K. Y., Van Zwieten, L., Meszaros, I., Downie, A., & Joseph, S. (2007). Agronomic values of greenwaste biochar as a soil amendment. *Australian Journal of Soil Research*, *45*(8), 629–634. https://doi.org/10.1071/SR07109

Chen, B., Zhou, D., & Zhu, L. (2008). Transitional adsorption and partition of nonpolar and polar aromatic contaminants by biochars of pine needles with different pyrolytic temperatures. *Environmental Science and Technology*, *42*(14), 5137–5143. https://doi.org/10.1021/es8002684

Chen, Y., Yang, H., Wang, X., Zhang, S., & Chen, H. (2012). Biomass-based pyrolytic polygeneration system on cotton stalk pyrolysis: Influence of temperature. *Bioresource Technology*, *107*, 411–418. https://doi.org/10.1016/j.biortech.2011.10.074

Chew, J. J., & Doshi, V. (2011). Recent advances in biomass pretreatment - Torrefaction fundamentals and technology. *Renewable and Sustainable Energy Reviews*, *15*(8), 4212–4222. https://doi.org/10.1016/j.rser.2011.09.017

Demirbas, A. (2004). Effects of temperature and particle size on bio-char yield from pyrolysis of agricultural residues. *Journal of Analytical and Applied Pyrolysis*, *72*(2), 243–248. https://doi.org/10.1016/j.jaap.2004.07.003

Dijkstra, J. J., Meeussen, J. C. L., & Comans, R. N. J. (2004). Leaching of heavy metals from contaminated soils: An experimental and modeling study. *Environmental Science and Technology*, *38*(16), 4390–4395. https://doi.org/10.1021/es049885v

Ding, W., Dong, X., Ime, I. M., Gao, B., & Ma, L. Q. (2014). Pyrolytic temperatures impact lead sorption mechanisms by bagasse biochars. *Chemosphere*, *105*, 68–74. https://doi.org/10.1016/j.chemosphere.2013.12.042

Do, D. (1998). Adsorption Analysis: Equilibria and Kinetics. *Imperial College Press*, *2*, 337–414. https://doi.org/10.1142/9781860943829_0007

Do, X. H., & Lee, B. K. (2013). Removal of Pb2+ using a biochar-alginate capsule in aqueous solution and capsule regeneration. *Journal of Environmental Management*, *131*, 375–382. https://doi.org/10.1016/j.jenvman.2013.09.045

Eccles, H. (1999). Treatment of metal-contaminated wastes: Why select a biological process? *Trends in Biotechnology*, *17*(12), 462–465. https://doi.org/10.1016/S0167-7799(99)01381-5

Fang, J., Gao, B., Zimmerman, A. R., Ro, K. S., & Chen, J. (2016). Physically (CO2) activated hydrochars from hickory and peanut hull: Preparation, characterization, and sorption of methylene blue, lead, copper, and cadmium. *RSC Advances*, *6*(30), 24906–24911. https://doi.org/10.1039/c6ra01644h

Gaskin, J. W., Steiner, C., Harris, K., Das, K. C., & Bibens, B. (2008). Effect of Low-Temperature Pyrolysis Conditions on Biochar for Agricultural Use. *Transactions of the ASABE*, *51*(6), 2061–2069. https://doi.org/10.13031/2013.25409

Gedam, A. H., & Dongre, R. S. (2019). Comparative study of sponge gourd derived biochar and activated carbon for bio-sorption and desorption of Pb(II) ions. *Materials Today: Proceedings*, *18*, 887–900. https://doi.org/10.1016/j.matpr.2019.06.521

Gotoh, T., Matsushima, K., & Kikuchi, K. I. (2004). Preparation of alginate-chitosan hybrid gel beads and adsorption of divalent metal ions. *Chemosphere*, *55*(1), 135–140. https://doi.org/10.1016/j.chemosphere.2003.11.016

Haghseresht, F., & Lu, G. Q. (1998). Adsorption characteristics of phenolic compounds onto coal-reject-derived adsorbents. *Energy and Fuels*, *12*(6), 1100–1107. https://doi.org/10.1021/ef9801165

Hall, K. R., Eagleton, L. C., Acrivos, A., & Vermeulen, T. (1966). Pore- and solid-diffusion kinetics in fixed-bed adsorption under constant-pattern conditions. *Industrial and Engineering Chemistry Fundamentals*, *5*(2), 212–223. https://doi.org/10.1021/i160018a011

Haney, R. L., Haney, E. B., White, M. J., & Smith, D. R. (2018). Soil CO2 response to organic and amino acids. *Applied Soil Ecology*, *125*(September 2017), 297–300. https://doi.org/10.1016/j.apsoil.2017.12.016

Hannam, K. D., Venier, L., Allen, D., Deschamps, C., Hope, E., Jull, M., Kwiaton, M., McKenney, D., Rutherford, P. M., & Hazlett, P. W. (2018). Wood ash as a soil amendment in Canadian forests: What are the barriers to utilization? *Canadian Journal of Forest Research*, *48*(4), 442–450. https://doi.org/10.1139/cjfr-2017-0351

Health Canada. (2019). Guidelines for Canadian Drinking Water Quality. In *National Meeting - American Chemical Society, Division of Environmental Chemistry* (Vol. 24, Issue 2). https://doi.org/10.1021/ba-1987-0214.ch035

Health Canada. (2020). Guidelines for Canadian Drinking Water Quality. *Water and Air Quality Bureau, Healthy Environments and Consumer Safety Branch, Health Canada*, *September 2020*, 25.

Ho, Y. S., Huang, C. T., & Huang, H. W. (2002). Equilibrium sorption isotherm for metal ions on tree fern. *Process Biochemistry*, *37*(12), 1421–1430. https://doi.org/10.1016/S0032-9592(02)00036-5

Inyang, M., Gao, B., Pullammanappallil, P., Ding, W., & Zimmerman, A. R. (2010). Biochar from anaerobically digested sugarcane bagasse. *Bioresource Technology*, *101*(22), 8868–8872. https://doi.org/10.1016/j.biortech.2010.06.088

Inyang, M., Gao, B., Yao, Y., Xue, Y., Zimmerman, A., Mosa, A., Pullammanappallil, P., Ok, Y. S., & Cao, X. (2016). A review of biochar as a low-cost adsorbent for aqueous heavy metal removal. *Critical Reviews in Environmental Science and Technology*, *46*(4), 406–433. https://doi.org/10.1080/10643389.2015.1096880

Issabayeva, G., Aroua, M. K., & Sulaiman, N. M. N. (2006). Removal of lead from aqueous solutions on palm shell activated carbon. *Bioresource Technology*, *97*(18), 2350–2355. https://doi.org/10.1016/j.biortech.2005.10.023

Jones, D. L., & Quilliam, R. S. (2014). Metal contaminated biochar and wood ash negatively affect plant growth and soil quality after land application. *Journal of Hazardous Materials*, *276*, 362–370. https://doi.org/10.1016/j.jhazmat.2014.05.053

Joseph, S. D., Camps-Arbestain, M., Lin, Y., Munroe, P., Chia, C. H., Hook, J., Van Zwieten, L., Kimber, S., Cowie, A., Singh, B. P., Lehmann, J., Foidl, N., Smernik, R. J., & Amonette, J. E. (2010). An investigation into the reactions of biochar in soil. *Australian Journal of Soil Research*, *48*(6–7), 501–515. https://doi.org/10.1071/SR10009

Langmuir, I. (1918). The adsorption of gases on plane surfaces of glass, mica and platinum. *Journal of the American Chemical Society*, *40*(9), 1361–1403.

Lee, K. Y., & Mooney, D. J. (2012). Alginate: Properties and biomedical applications. *Progress in Polymer Science (Oxford)*, *37*(1), 106–126. https://doi.org/10.1016/j.progpolymsci.2011.06.003

Lehmann, J. (2007a). A Handful of Carbon. *Nature*, *447*(May 10), 143–144.

Lehmann, J. (2007b). Bio-Energy in the Black. *Frontiers in Ecology and the Environment*, *5*(September), 381–387. http://www.jstor.org/stable/20440704%0Ahttp://about.jstor.org/terms%0Ahttp://discovery.ucl.ac.uk/1322126/

Lehmann, J., Gaunt, J., & Rondon, M. (2006). Bio-char sequestration in terrestrial ecosystems - A review. *Mitigation and Adaptation Strategies for Global Change*, *11*(2), 403–427. https://doi.org/10.1007/s11027-005-9006-5

Lehmann, J., & Joseph, S. (2009). An introduction. In *Biochar for Environmental Management: Science and Technology* (Issue 2009). https://doi.org/10.4324/9781849770552

Lehmann, J., Rillig, M. C., Thies, J., Masiello, C. A., Hockaday, W. C., & Crowley, D. (2011). Biochar effects on soil biota - A review. *Soil Biology and Biochemistry*, *43*(9), 1812–1836. https://doi.org/10.1016/j.soilbio.2011.04.022

Liang, B., Lehmann, J., Solomon, D., Kinyangi, J., Grossman, J., O'Neill, B., Skjemstad, J. O., Thies, J., Luizão, F. J., Petersen, J., & Neves, E. G. (2006). Black Carbon Increases Cation Exchange Capacity in Soils. *Soil Science Society of America Journal*, *70*(5), 1719–1730. https://doi.org/10.2136/sssaj2005.0383

Liu, C., Ye, J., Lin, Y., Wu, J., Price, G. W., Burton, D., & Wang, Y. (2020). Removal of Cadmium (II) using water hyacinth (Eichhornia crassipes) biochar alginate beads in aqueous solutions. *Environmental Pollution*, *264*, 114785. https://doi.org/10.1016/j.envpol.2020.114785

Liu, Z., & Zhang, F. S. (2009). Removal of lead from water using biochars prepared from hydrothermal liquefaction of biomass. *Journal of Hazardous Materials*, *167*(1–3), 933–939. https://doi.org/10.1016/j.jhazmat.2009.01.085

Lucchini, P., Quilliam, R. S., DeLuca, T. H., Vamerali, T., & Jones, D. L. (2014). Increased bioavailability of metals in two contrasting agricultural soils treated with waste wood-derived biochar and ash. *Environmental Science and Pollution Research*, *21*(5), 3230–3240. https://doi.org/10.1007/s11356-013-2272-y

Montes-Morán, M. A., Suárez, D., Menéndez, J. A., & Fuente, E. (2004). On the nature of basic sites on carbon surfaces: An overview. *Carbon*, *42*(7), 1219–1225. https://doi.org/10.1016/j.carbon.2004.01.023

Mukherjee, A., Zimmerman, A. R., & Harris, W. (2011). Surface chemistry variations among a series of laboratory-produced biochars. *Geoderma*, *163*(3–4), 247–255. https://doi.org/10.1016/j.geoderma.2011.04.021

Mukome, Fu., Zhang, X., Silva, L., Six, J., & Parikh, S. (2014). Use of Chemical and Physical Characteristics to Investiage Trends in Biochar Feedstock. *J Agric Food Chem*, *61*(9), 2196–2204. https://doi.org/10.1038/jid.2014.371

Nandi, B. K., Goswami, A., & Purkait, M. K. (2009). Adsorption characteristics of brilliant green dye on kaolin. *Journal of Hazardous Materials*, *161*(1), 387–395. https://doi.org/10.1016/j.jhazmat.2008.03.110

Novak, J., Lima, I., Xing, B., Steiner, C., Das, K. C., Ahmedna, M., Rehrah, D., Watts, D., Busscher, W., & Schomberg, H. (2009). Characterization of Designer Biochar Produced at Different Temperatures and their Effects on a Loamy Sand. *Annals of Environemntal Science*, *3*, 195–206.

Osmari, T. A., Gallon, R., Schwaab, M., Barbosa-Coutinho, E., Severo, J. B., & Pinto, J. C. (2013). Statistical analysis of linear and non-linear regression for the estimation of adsorption isotherm parameters. *Adsorption Science and Technology*, *31*(5), 433–458. https://doi.org/10.1260/0263-6174.31.5.433

Pugliese, S., Jones, T., Preston, M. D., Hazlett, P., Tran, H., & Basiliko, N. (2014). Wood ash as a forest soil amendment: The role of boiler and soil type on soil property response. *Canadian Journal of Soil Science*, *94*(5), 621–634. https://doi.org/10.4141/cjss-2014-037

Rajapaksha, A. U., Chen, S. S., Tsang, D. C. W., Zhang, M., Vithanage, M., Mandal, S., Gao, B., Bolan, N. S., & Ok, Y. S. (2016). Engineered/designer biochar for contaminant removal/immobilization from soil and water: Potential and implication of biochar modification. *Chemosphere*, *148*, 276–291. https://doi.org/10.1016/j.chemosphere.2016.01.043

Rees, F., Simonnot, M. O., & Morel, J. L. (2014). Short-term effects of biochar on soil heavy metal mobility are controlled by intra-particle diffusion and soil pH increase. *European Journal of Soil Science*, *65*(1), 149–161. https://doi.org/10.1111/ejss.12107

Renu, M. A., Singh, K., Upadhyaya, S., & Dohare, R. K. (2017). Removal of heavy metals from wastewater using modified agricultural adsorbents. *Materials Today: Proceedings*, *4*(9), 10534–10538. https://doi.org/10.1016/j.matpr.2017.06.415

Roh, H., Yu, M. R., Yakkala, K., Koduru, J. R., Yang, J. K., & Chang, Y. Y. (2015). Removal studies of Cd(II) and explosive compounds using buffalo weed biochar-alginate beads. *Journal of Industrial and Engineering Chemistry*, *26*, 226–233. https://doi.org/10.1016/j.jiec.2014.11.034

Ronsse, F., van Hecke, S., Dickinson, D., & Prins, W. (2013). Production and characterization of slow pyrolysis biochar: Influence of feedstock type and pyrolysis conditions. *GCB Bioenergy*, *5*(2), 104–115. https://doi.org/10.1111/gcbb.12018

Service United States Department of Agriculture Natural Resources Conservation. (2014). Soil Respiration: Soil Healt - Guides for Educators. In *USDA-NRCS* (Issue May, pp. 1–8).

Shaaban, A., Se, S. M., Dimin, M. F., Juoi, J. M., Mohd Husin, M. H., & Mitan, N. M. M. (2014). Influence of heating temperature and holding time on biochars derived from rubber wood sawdust via slow pyrolysis. *Journal of Analytical and Applied Pyrolysis*, *107*, 31–39. https://doi.org/10.1016/j.jaap.2014.01.021

Shinogi, Y., & Kanri, Y. (2003). Pyrolysis of plant, animal and human waste: Physical and chemical characterization of the pyrolytic products. *Bioresource Technology*, *90*(3), 241–247. https://doi.org/10.1016/S0960-8524(03)00147-0

Singh, B., Singh, B. P., & Cowie, A. (2010). Characterisation and evaluation of biochars for their application as a soil amendment. *Australian Journal of Soil Research*, *48*, 516–525. https://doi.org/10.1071/SR10058 0004-9573/10/070516

Sohi, S. P., Krull, E., Lopez-Capel, E., & Bol, R. (2010). A review of biochar and its use and function in soil. In *Advances in Agronomy* (Vol. 105, Issue 1). https://doi.org/10.1016/S0065-2113(10)05002-9

Song, W., & Guo, M. (2012). Quality variations of poultry litter biochar generated at different pyrolysis temperatures. *Journal of Analytical and Applied Pyrolysis*, *94*, 138–145. https://doi.org/10.1016/j.jaap.2011.11.018

Srinivasan, P., Sarmah, A. K., Smernik, R., Das, O., Farid, M., & Gao, W. (2015). A feasibility study of agricultural and sewage biomass as biochar, bioenergy and biocomposite feedstock: Production, characterization and potential applications. *Science of the Total Environment*, *512–513*, 495–505. https://doi.org/10.1016/j.scitotenv.2015.01.068

Steinbeiss, S., Gleixner, G., & Antonietti, M. (2009). Effect of biochar amendment on soil carbon balance and soil microbial activity. *Soil Biology and Biochemistry*, *41*(6), 1301–1310. https://doi.org/10.1016/j.soilbio.2009.03.016

Suliman, W., Harsh, J. B., Abu-Lail, N. I., Fortuna, A. M., Dallmeyer, I., & Garcia-Perez, M. (2016). Influence of feedstock source and pyrolysis temperature on biochar bulk and surface properties. *Biomass and Bioenergy*, *84*, 37–48. https://doi.org/10.1016/j.biombioe.2015.11.010

Sun, Y., Gao, B., Yao, Y., Fang, J., Zhang, M., Zhou, Y., Chen, H., & Yang, L. (2014). Effects of feedstock type, production method, and pyrolysis temperature on biochar and hydrochar properties. *Chemical Engineering Journal*, *240*, 574–578. https://doi.org/10.1016/j.cej.2013.10.081

Sweeney, E., Yu, Z. M., Parker, L., & Dummer, T. J. B. (2017). Lead in drinking water: a response from the Atlantic PATH study. *Environmental Health Review*, *60*(1), 9–13. https://doi.org/10.5864/d2017-002

Tag, A. T., Duman, G., Ucar, S., & Yanik, J. (2016). Effects of feedstock type and pyrolysis temperature on potential applications of biochar. *Journal of Analytical and Applied Pyrolysis*, *120*, 200–206. https://doi.org/10.1016/j.jaap.2016.05.006

Tomczyk, A., Sokołowska, Z., & Boguta, P. (2020). Biochar physicochemical properties: pyrolysis temperature and feedstock kind effects. *Reviews in Environmental Science and Biotechnology*, *19*(1), 191–215. https://doi.org/10.1007/s11157-020-09523-3

Uchimiya, M., Chang, S. C., & Klasson, K. T. (2011a). Screening biochars for heavy metal retention in soil: Role of oxygen functional groups. *Journal of Hazardous Materials*, *190*(1–3), 432–441. https://doi.org/10.1016/j.jhazmat.2011.03.063

Uchimiya, M., Wartelle, L. H., Klasson, K. T., Fortier, C. A., & Lima, I. M. (2011b). Influence of pyrolysis temperature on biochar property and function as a heavy metal sorbent in soil. *Journal of Agricultural and Food Chemistry*, *59*(6), 2501–2510. https://doi.org/10.1021/jf104206c

Van Zwieten, L., Kimber, S., Morris, S., Chan, K. Y., Downie, A., Rust, J., Joseph, S., & Cowie, A. (2010). Effects of biochar from slow pyrolysis of papermill waste on agronomic performance and soil fertility. *Plant and Soil*, *327*(1), 235–246. https://doi.org/10.1007/s11104-009-0050-x

Verheijen, F., Jeffery, S., Bastos, A. C., Van Der Velde, M., & Diafas, I. (2010). Biochar Application to Soils: A Critical Scientific Review of Effects on Soil Properties, Processes and Functions. In *Environment* (Vol. 8, Issue 4). https://doi.org/10.2788/472

Wang, B., Gao, B., & Fang, J. (2017). Recent advances in engineered biochar productions and applications. *Critical Reviews in Environmental Science and Technology*, *47*(22), 2158–2207. https://doi.org/10.1080/10643389.2017.1418580

Wang, B., Gao, B., & Wan, Y. (2018a). Comparative study of calcium alginate, ball-milled biochar, and their composites on aqueous methylene blue adsorption. *Environmental Science and Pollution Research*, *26*(12), 11535–11541. https://doi.org/10.1007/s11356-018-1497-1

Wang, B., Gao, B., & Wan, Y. (2018b). Entrapment of ball-milled biochar in Ca-alginate beads for the removal of aqueous Cd(II). *Journal of Industrial and Engineering Chemistry*, *61*, 161–168. https://doi.org/10.1016/j.jiec.2017.12.013

Wang, B., Gao, B., Zimmerman, A. R., Zheng, Y., & Lyu, H. (2018c). Novel biochar-impregnated calcium alginate beads with improved water holding and nutrient retention properties. *Journal of Environmental Management*, *209*, 105–111. https://doi.org/10.1016/j.jenvman.2017.12.041

Wang, Q., Wang, B., Lee, X., Lehmann, J., & Gao, B. (2018d). Sorption and desorption of Pb(II) to biochar as affected by oxidation and pH. *Science of the Total Environment*, *634*, 188–194. https://doi.org/10.1016/j.scitotenv.2018.03.189

Wang, L., Wang, Y., Ma, F., Tankpa, V., Bai, S., Guo, X., & Wang, X. (2019a). Mechanisms and reutilization of modified biochar used for removal of heavy metals from wastewater: A review. *Science of the Total Environment*, *668*, 1298–1309. https://doi.org/10.1016/j.scitotenv.2019.03.011

Wang, B., Wan, Y., Zheng, Y., Lee, X., Liu, T., Yu, Z., Huang, J., Ok, Y. S., Chen, J., & Gao, B. (2019b). Alginate-based composites for environmental applications: a critical review. *Critical Reviews in Environmental Science and Technology*, *49*(4), 318–356. https://doi.org/10.1080/10643389.2018.1547621

Wang, S., Gao, B., Zimmerman, A. R., Li, Y., Ma, L., Harris, W. G., & Migliaccio, K. W. (2015). Physicochemical and sorptive properties of biochars derived from woody and herbaceous biomass. *Chemosphere*, *134*, 257–262. https://doi.org/10.1016/j.chemosphere.2015.04.062

Wardle, D. A., Nilsson, M. C., & Zackrisson, O. (2008). Response to comment on "fire-derived charcoal causes loss of forest humus." *Science*, *321*(5894). https://doi.org/10.1126/science.1160750

Winsley, P. (2007). Biochar and bioenergy production for climate change mitigation. *Science And Technology*, *64*(1), 5–10. http://www.biochar-international.org/images/NZSR64_1_Winsley.pdf

Xu, X., Cao, X., Zhao, L., Zhou, H., & Luo, Q. (2014). Interaction of organic and inorganic fractions of biohcar with Pb(II) ion: Further elucidation of mecharnisms for Pb(II) removal by biochar. *RSC Advances*, *85*, 2–9. https://doi.org/DOI: 10.1039/c0xx00000x

Yang, F., Wang, B., Shi, Z., Li, L., Li, Y., Mao, Z., Liao, L., Zhang, H., & Wu, Y. (2021). Immobilization of heavy metals (Cd, Zn, and Pb) in different contaminated soils with swine manure biochar. *Environmental Pollutants and Bioavailability*, *33*(1), 55–65. https://doi.org/10.1080/26395940.2021.1916407

Yang, R. (1987). Gas Separation by Adsorption Processes. In *Chemical Engineering Science* (Vol. 43, Issue 4). https://doi.org/10.1016/0009-2509(88)80096-4

Yao, Y., Gao, B., Inyang, M., Zimmerman, A. R., Cao, X., Pullammanappallil, P., & Yang, L. (2011). Biochar derived from anaerobically digested sugar beet tailings: Characterization and phosphate removal potential. *Bioresource Technology*, *102*(10), 6273–6278. https://doi.org/10.1016/j.biortech.2011.03.006

Yao, Y., Gao, B., Zhang, M., Inyang, M., & Zimmerman, A. R. (2012). Effect of biochar amendment on sorption and leaching of nitrate, ammonium, and phosphate in a sandy soil. *Chemosphere*, *89*(11), 1467–1471. https://doi.org/10.1016/j.chemosphere.2012.06.002

Yu, H., Zhang, Z., Li, Z., & Chen, D. (2014). Characteristics of tar formation during cellulose, hemicellulose and lignin gasification. *Fuel*, *118*, 250–256. https://doi.org/10.1016/j.fuel.2013.10.080

Yuan, J. H., Xu, R. K., & Zhang, H. (2011). The forms of alkalis in the biochar produced from crop residues at different temperatures. *Bioresource Technology*, *102*(3), 3488–3497. https://doi.org/10.1016/j.biortech.2010.11.018

Zama, E. F., Zhu, Y. G., Reid, B. J., & Sun, G. X. (2017). The role of biochar properties in influencing the sorption and desorption of Pb(II), Cd(II) and As(III) in aqueous solution. *Journal of Cleaner Production*, *148*, 127–136. https://doi.org/10.1016/j.jclepro.2017.01.125

Zhang, F., Wang, X., Yin, D., Peng, B., Tan, C., Liu, Y., Tan, X., & Wu, S. (2015). Efficiency and mechanisms of Cd removal from aqueous solution by biochar derived from water hyacinth (Eichornia crassipes). *Journal of Environmental Management*, *153*, 68–73. https://doi.org/10.1016/j.jenvman.2015.01.043

Zhang, Y., Price, G. W., Jamieson, R., Burton, D., & Khosravi, K. (2017). Sorption and desorption of selected non-steroidal anti-inflammatory drugs in an agricultural loam-textured soil. *Chemosphere*, *174*, 628–637. https://doi.org/10.1016/j.chemosphere.2017.02.027

Zhang, Z., Zhu, Z., Shen, B., & Liu, L. (2019). Insights into biochar and hydrochar production and applications: A review. *Energy*, *171*, 581–598. https://doi.org/10.1016/j.energy.2019.01.035

Zheng, W., Guo, M., Chow, T., Bennett, D. N., & Rajagopalan, N. (2010). Sorption properties of greenwaste biochar for two triazine pesticides. *Journal of Hazardous Materials*, *181*(1–3), 121–126. https://doi.org/10.1016/j.jhazmat.2010.04.103

Zimmermann, S., & Frey, B. (2002). Soil respiration and microbial properties in an acid forest soil: Effects of wood ash. *Soil Biology and Biochemistry*, *34*(11), 1727–1737. https://doi.org/10.1016/S0038-0717(02)00160-8

Appendix: Additional Experimental Data

Table 7. Experimental adsorption data (μg g^{-1}) of the various biochar and BAC treatments at each Pb^{2+} concentration from the first chapter (n=3).

Pb^{2+} concentration (μg L^{-1})	Adsorption Capacity (μg g^{-1}) Treatment		
	B3[1]	B7[2]	BAC[3]
5	4.67 ± 0.1	5.01 ± 0.0	4.39 ± 0.0
12	6.03 ± 0.1	10.1 ± 0.0	11.0 ± 0.3
28	18.6 ± 3.0	26.5 ± 0.5	26.7 ± 0.0
50	43.7 ± 0.5	48.0 ± 0.6	49.2 ± 0.0
62	59.4 ± 0.8	61.3 ± 0.2	61.2 ± 0.0
94	88.4 ± 0.5	91.5 ± 0.5	91.1 ± 0.4

[1]B3 biochar with an adsorption time of 3 days
[2]B7 biochar with an adsorption time of 7 days
[3]BAC biochar-alginate composite with an adsorption time of 1 day

Table 8. Experimental desorption data (μg g^{-1}) of the various biochar and BAC treatments at each Pb^{2+} concentration from the first chapter (n=3).

Pb^{2+} concentration (μg L^{-1})	Desorption Capacity (μg g^{-1}) Treatment				
	B3D3[1]	B3D7[2]	B7D3[3]	B7D7[4]	BACD[5]
5	4.32 ± 0.7	3.85 ± 0.2	2.73 ± 0.1	3.40 ± 0.3	3.71 ± 1.2
12	10.1 ± 0.6	9.11 ± 0.8	8.47 ± 0.6	9.43 ± 0.3	10.4 ± 0.5
28	21.9 ± 0.0	19.7c ± 1.6	13.2 ± 3.2	19.0 ± 2.7	25.0 ± 1.2
50	29.2 ± 0.5	27.5 ±1.4	30.2 ± 4.4	29.5 ± 0.2	32.6 ± 1.2
62	36.8 ± 0.8	38.0 ± 3.0	37.7 ± 1.0	35.0 ± 8.8	45.2 ± 0.6
94	70.3 ± 0.5	64.7 ± 5.5	73.5 ± 6.6	77.7 ± 0.5	86.3 ± 2.8

[1]B3D3 biochar with an adsorption and desorption time of 3 days
[2]B3D3 biochar with an adsorption and desorption time of 3 and 7 days, respectively
[3]B7D3 biochar with an adsorption and desorption time of 7 and 3 days, respectively
[4]B7D7 biochar with an adsorption and desorption time of 7 days
[5]BACD biochar-alginate composite with an adsorption and desorption time of 1 day